

# Supplementary Information for: Ecosystem size and complexity dictate riverine biodiversity

Akira Terui\*      Seoghyun Kim\*      Christine L. Dolph<sup>†</sup>      Taku Kadoya<sup>‡</sup>  
Yusuke Miyazaki<sup>§</sup>

## Contents

<b>Theory</b>	<b>1</b>
Sensitivity analysis . . . . .	1
Longitudinal gradients of local species richness . . . . .	2
<b>Empirical data</b>	<b>2</b>
Fish community data . . . . .	2
<b>Tables</b>	<b>4</b>
Table S1 Simulation parameter (sensitivity analysis) . . . . .	4
Table S2 Simulation parameter (main analysis) . . . . .	5
Table S3 Sensitivity analysis for the effect of ecosystem size . . . . .	6
Table S4 Sensitivity analysis for the effect of ecosystem complexity . . . . .	7
Table S5 List of fish species in Hokkaido, Japan . . . . .	8
Table S6 List of fish species in Midwest, US . . . . .	10
<b>Figures</b>	<b>14</b>
Figure S1 Longitudinal gradient of local species richness ( $\sigma_h = 1, \sigma_l = 0.01$ ) . . . . .	14
Figure S2 Longitudinal gradient of local species richness ( $\sigma_h = 1, \sigma_l = 1$ ) . . . . .	15
Figure S3 Longitudinal gradient of local species richness ( $\sigma_h = 0.01, \sigma_l = 0.01$ ) . . . . .	16
Figure S4 Longitudinal gradient of local species richness ( $\sigma_h = 0.01, \sigma_l = 1$ ) . . . . .	17
Figure S5 Influence of ecosystem size ( $p_d = 0.1, \sigma_h = 1, \sigma_l = 0.01$ ) . . . . .	18
Figure S6 Influence of ecosystem size ( $p_d = 0.1, \sigma_h = 1, \sigma_l = 1$ ) . . . . .	19
Figure S7 Influence of ecosystem size ( $p_d = 0.1, \sigma_h = 0.01, \sigma_l = 0.01$ ) . . . . .	20
Figure S8 Influence of ecosystem size ( $p_d = 0.1, \sigma_h = 0.01, \sigma_l = 1$ ) . . . . .	21
Figure S9 Influence of ecosystem size ( $p_d = 0.01, \sigma_h = 1, \sigma_l = 1$ ) . . . . .	22
Figure S10 Influence of ecosystem size ( $p_d = 0.01, \sigma_h = 0.01, \sigma_l = 0.01$ ) . . . . .	23
Figure S11 Influence of ecosystem size ( $p_d = 0.01, \sigma_h = 0.01, \sigma_l = 1$ ) . . . . .	24
Figure S12 Influence of ecosystem complexity ( $p_d = 0.1, \sigma_h = 1, \sigma_l = 0.01$ ) . . . . .	25
Figure S13 Influence of ecosystem complexity ( $p_d = 0.1, \sigma_h = 1, \sigma_l = 1$ ) . . . . .	26
Figure S14 Influence of ecosystem complexity ( $p_d = 0.1, \sigma_h = 0.01, \sigma_l = 0.01$ ) . . . . .	27
Figure S15 Influence of ecosystem complexity ( $p_d = 0.1, \sigma_h = 0.01, \sigma_l = 1$ ) . . . . .	28
Figure S16 Influence of ecosystem complexity ( $p_d = 0.01, \sigma_h = 1, \sigma_l = 1$ ) . . . . .	29
Figure S17 Influence of ecosystem complexity ( $p_d = 0.01, \sigma_h = 0.01, \sigma_l = 0.01$ ) . . . . .	30
Figure S18 Influence of ecosystem complexity ( $p_d = 0.01, \sigma_h = 0.01, \sigma_l = 1$ ) . . . . .	31

---

\*Department of Biology, University of North Carolina at Greensboro

<sup>†</sup>Department of Ecology, Evolution and Behavior, University of Minnesota

<sup>‡</sup>National Institute for Environmental Studies

<sup>§</sup>Shiraume Gakuen University

## Theory

### Sensitivity analysis

We performed a sensitivity analysis of the metacommunity simulation to identify key simulation parameters that strongly affect the relationships between diversity metrics ( $\alpha$ ,  $\beta$ , and  $\gamma$ ) and ecosystem properties (the number of habitat patches  $N_p$  and branching probability  $P_b$ ). We generated 500 sets of parameter combinations by randomly drawing values of 8 simulation parameters from uniform distributions (**Table S1**). For each parameter combination, we generated 100 branching networks with the gradients of ecosystem size ( $N_p \sim Unif(10, 150)$ ) and complexity ( $P_b \sim Unif(0.01, 0.99)$ ). This results in a total of 50000 simulation replicates. In each simulation replicate, we allowed interspecific variation in niche optimum  $\mu_i$  and width  $\sigma_{niche,i}$  ( $\mu_i \sim Unif(-1, 1)$  and  $\sigma_{niche,i} \sim Unif(0.1, 1)$ , respectively; subscript  $i$  represents species) and ran 1400 time steps of metacommunity dynamics. We obtained temporal means of  $\alpha$ ,  $\beta$ , and  $\gamma$  diversity for the last 1000 time steps. The first 400 time steps were discarded as initialization and burn-in periods.

For each parameter combination, we regressed log-transformed  $\alpha$ ,  $\beta$ , and  $\gamma$  diversity ( $\log_{10} y_j$  for network replicate  $j$ ) on the number of habitat patches  $N_p$  and branching probability  $P_b$  as:

$$\log_{10} y_j \sim Normal(\mu_j, \sigma^2)$$

$$\mu_j = \psi_0 + \psi_1 \log_{10} N_{p,j} + \psi_2 \log_{10} P_{b,j}$$

where  $\psi_q$  ( $q = 0 - 2$ ) are the intercept ( $\psi_0$ ) and regression coefficients ( $\psi_1$  and  $\psi_2$ ). We extracted 500 estimates of  $\psi_1$  and  $\psi_2$ , which represent the effects of  $N_p$  and  $P_b$  on diversity metrics under a given parameter combination. To examine influences of simulation parameters (**Table S1**) on  $\psi_1$  and  $\psi_2$ , we developed the following regression model taking  $\psi_1$  or  $\psi_2$  as a dependent variable  $u_k$  (parameter combination  $k$ ):

$$u_k \sim Normal(\mu_k, \sigma^2)$$

$$\mu_k = \zeta_0 + \zeta_1 \sigma_{h,k} + \zeta_2 \sigma_{l,k} + \zeta_3 \sigma_{z,k} + \zeta_4 \phi_k + \zeta_5 \nu_k + \zeta_6 \alpha_{max,k} + \zeta_7 \theta_k + \zeta_8 p_{d,k}$$

where  $\zeta_q$  ( $q = 0 - 8$ ) are the intercept and regression coefficients. Explanatory variables were standardized to a mean of zero and a standard deviation of one, so that regression coefficients are comparable.

The sensitivity analysis revealed key simulation parameters. For the effects of  $N_p$ , the following simulation parameters were influential: the degree of local environmental noise ( $\sigma_l$ ; influenced the effects on  $\alpha$  and  $\gamma$  diversity), the maximum value of interspecific competition coefficient ( $\alpha_{max}$ ; influenced the effects on  $\alpha$ ,  $\beta$ , and  $\gamma$  diversity), dispersal distance ( $\theta$ ; influenced the effects on  $\alpha$  and  $\beta$  diversity), and dispersal probability ( $p_d$ ; influenced the effect on  $\alpha$  diversity) (**Table S3**). For the effects of  $P_b$ , the following simulation parameters were influential: environmental variation at headwaters ( $\sigma_h$ ; influenced the effect on  $\gamma$  diversity), the degree of local environmental noise ( $\sigma_l$ ; influenced the effects on  $\alpha$  and  $\beta$  diversity), and dispersal distance ( $\theta$ ; influenced the effects on  $\alpha$  and  $\beta$  diversity) (**Table S4**).

Based on the results, we identified  $\sigma_h$ ,  $\sigma_l$ ,  $\alpha_{max}$ ,  $\theta$ , and  $p_d$  as key parameters. We changed the values of these parameters in the main analysis and examined the relationships between diversity metrics and ecosystem properties.

### Longitudinal gradients of local species richness

Longitudinal gradients of local species richness have been extensively studied in rivers, illuminating typical patterns observed in nature. The most common pattern is a downstream increase of local species richness<sup>1-4</sup>. However, recent empirical and theoretical studies also showed ‘reversed patterns,’ in which local species richness decreases downstream<sup>5,6</sup>. We predicted the longitudinal gradient of local species richness to confirm

that our simulation scenarios are capable of reproducing the previously observed patterns of local species richness. We considered 32 simulation scenarios comprising four landscape and eight ecological scenarios, as described in the main text (a set of parameters is described in **Table S2**). Under each simulation scenario, we generated 10 branching networks with fixed parameters of ecosystem size ( $N_p = 100$ ) and complexity ( $P_b = 0.5$ ). This results in a total of 320 simulation replicates. In each simulation replicate, we allowed interspecific variation in niche optimum  $\mu_i$  and width  $\sigma_{niche,i}$  ( $\mu_i \sim Unif(-1, 1)$  and  $\sigma_{niche,i} \sim Unif(0.1, 1)$ , respectively; subscript  $i$  represents species) and ran 1400 time steps of metacommunity dynamics. We obtained temporal means of local species richness at each habitat patch for the last 1000 time steps. The first 400 time steps were discarded as initialization and burn-in periods. We evaluated the relationship between local species richness and the number of upstream habitat patches, a proxy for the longitudinal position of a habitat patch.

The simulation reproduced diverse patterns of longitudinal gradients in local species richness (**Figures S1-4**). The downstream increase of local species richness was predicted under a natural landscape scenario, in which environmental variation at headwaters  $\sigma_h$  exceeds the degree of local environmental noise  $\sigma_l$  (**Figure S1**). This pattern was consistent across ecological scenarios except those with long dispersal distance and high dispersal probability (**Figure S1**). Similarly, we observed a downstream increase of local species richness in scenarios with low habitat diversity ( $\sigma_h = \sigma_l = 0.01$ ) and low dispersal probability ( $p_d = 0.01$ ) (**Figure S3**). However, there were cases where local species richness decreased downstream or showed no longitudinal patterns. For example, when local environmental noise exceeds environmental variation at headwaters ( $\sigma_l \geq \sigma_h$ ), local species richness showed a downstream decrease or a vague longitudinal pattern (**Figure S4**). Therefore, the simulation scenarios were capable of reproducing previously observed patterns, suggesting the appropriateness in the choice of parameter combinations.

## Empirical data

### Fish community data

**Hokkaido, Japan.** We used data from the Hokkaido Freshwater Fish Database HFish<sup>7,8</sup>, monitoring data at protected watersheds<sup>9,10</sup>, and primary data collected by the authors<sup>4,11</sup>, which collectively cover the entire Hokkaido island. Fish data were collected from summer to fall. We screened data through the following procedure:

1. We listed recorded fish species and re-organized species names to be consistent across data sources. We removed the following species at this stage: (1) identified at the family-level; (2) marine fish species (including species that occasionally use brackish/freshwater habitats).
2. We selected sampling sites based on the following criteria: (1) surveys were conducted with netting and/or electrofishing, (2) surveys were designed to collect a whole fish community, (3) sites contained reliable coordinates (sites with coordinates identical at 3 decimal degrees were treated as the same site), and (4) sites did not involve species identified at the genus level that are rarely observed in the data set ( $< 100$  sites occurrence).
3. For sites with multiple visits (i.e., temporal replicates), we used the latest-year observation at each sampling site to minimize variation in sampling efforts among sites. Surveys that occurred in the same year were aggregated into a single observation.
4. We confined sites to those with the latest observation year of  $\geq 1990$ . Although the data set contained observations from 1953, we added this restriction to align the observation period with the data set in the Midwest, US.
5. Four genera (*Lethenteron*, *Pungitius*, *Rhinogobius*, and *Tribolodon*) were treated as species groups (i.e., spp.) as their taxonomic resolutions varied greatly among data sources due to difficulties in identifying species.

**Midwest, US.** We assembled fish community data collected by the Iowa Department of Natural Resources, Illinois Environmental Protection Agency and Illinois Department of Natural Resources, Minnesota Pollution Control Agency, and Wisconsin Department of Natural Resources. These data sets cover most of Upper Mississippi (Hydrologic Unit Code 2 [HUC 2], region 07, as defined by U.S. Geological Survey and U.S.

Department of Agriculture Natural Resources Conservation Service<sup>12</sup>) and the part of Great Lakes (HUC 2, region 04), Missouri (HUC 2, region 10), and Ohio (HUC 2, region 05). Fish data were collected from summer to fall with electrofishing (backpack, barge-type, or boat-mounted) and supplemental netting at some locations. We screened data through the following procedure:

1. We used data of the Upper Mississippi (HUC 2, region 07) and Great Lakes basins (HUC 2, region 04) as most sites are included in these regions.
2. We removed records of unidentified species, hybrid species, and commercial species apparently absent in the wild (e.g., goldfish).
3. We used the latest observation at each sampling site to minimize variation in sampling efforts among sites.

## Tables

**Table S1 Simulation parameter (sensitivity analysis)**

**Table S1** Parameter values used in the sensitivity analysis of the metacommunity simulation. See the main text for model details.

Parameter	Value	Interpretation
$\sigma_h$	Unif(0.01, 1)	Environmental variation at headwaters
$\sigma_l$	Unif(0.01, 1)	Degree of local environmental noise
$\sigma_z$	Unif(0.01, 0.5)	Temporal environmental variability
$\rho$	1	Strength of spatial autocorrelation in mean environmental condition
$\phi$	Unif(0.01, 1)	Extent of spatial autocorrelation in temporal environmental variation
$\nu$	Unif(1, 5)	Cost of a wider niche
$\alpha_{max}$	Unif(0.5, 1.5)	Maximum value of interspecific competition coefficient
$\theta$	Unif(0.1, 1)	Rate parameter of an exponential dispersal kernel
$p_d$	Unif(0.01, 0.1)	Dispersal probability
$r_{0,i}$	4	Maximum reproductive rate

## Table S2 Simulation parameter (main analysis)

**Table S2** Values and interpretation of simulation parameters used in the main simulation. See the main text for model details.

Parameter	Value	Interpretation
$\sigma_h$	0.01, 1.00	Environmental variation at headwaters
$\sigma_l$	0.01, 1.00	Degree of local environmental noise
$\sigma_z$	0.1	Temporal environmental variability
$\rho$	1	Strength of spatial autocorrelation in mean environmental condition
$\phi$	0.05	Extent of spatial autocorrelation in temporal environmental variation
$\nu$	1	Cost of a wider niche
$\alpha_{max}$	0.75, 1.50	Maximum value of interspecific competition coefficient
$\theta$	0.1, 1.0	Rate parameter of an exponential dispersal kernel
$p_d$	0.01, 0.10	Dispersal probability
$r_{0,i}$	4	Maximum reproductive rate

### Table S3 Sensitivity analysis for the effect of ecosystem size

**Table S3** Sensitivity analysis of the metacommunity simulation. Parameter estimates of linear regression models (standard errors in parenthesis) are shown. Dependent variables are the effects of the number of habitat patches ( $N_p$ ) on  $\alpha$ ,  $\beta$ , and  $\gamma$  diversity. Explanatory variables (i.e., simulation parameters) were standardized to a mean of zero and a standard deviation of one prior to the analysis. See Tables S1 and S2 for interpretation of the simulation parameters.

	<i>Dependent variable:</i>		
	Effect of $N_p$ on $\alpha$ diversity	Effect of $N_p$ on $\beta$ diversity	Effect of $N_p$ on $\gamma$ diversity
$\sigma_h$	0.008*** (0.002)	-0.003** (0.001)	0.005*** (0.002)
$\sigma_l$	-0.021*** (0.002)	0.004*** (0.001)	-0.018*** (0.002)
$\sigma_z$	0.0001 (0.002)	-0.013*** (0.001)	-0.013*** (0.002)
$\phi$	0.001 (0.002)	-0.0002 (0.001)	0.0003 (0.002)
$\nu$	-0.001 (0.002)	-0.009*** (0.001)	-0.009*** (0.002)
$\alpha_{max}$	0.019*** (0.002)	0.028*** (0.001)	0.047*** (0.002)
$\theta$	-0.040*** (0.002)	0.041*** (0.001)	0.001 (0.002)
$p_d$	0.017*** (0.002)	-0.006*** (0.001)	0.010*** (0.002)
Intercept	0.147*** (0.002)	0.137*** (0.001)	0.284*** (0.002)
$R^2$	0.583	0.759	0.644

*Note:*

\*p<0.1; \*\*p<0.05; \*\*\*p<0.01

## Table S4 Sensitivity analysis for the effect of ecosystem complexity

**Table S4** Sensitivity analysis of the metacommunity simulation. Parameter estimates of linear regression models (standard errors in parenthesis) are shown. Dependent variables are the effects of branching probability ( $P_b$ ) on  $\alpha$ ,  $\beta$ , and  $\gamma$  diversity. Explanatory variables (i.e., simulation parameters) were standardized to a mean of zero and a standard deviation of one prior to the analysis. See Tables S1 and S2 for interpretation of the simulation parameters.

	<i>Dependent variable:</i>		
	Effect of $P_b$ on $\alpha$ diversity	Effect of $P_b$ on $\beta$ diversity	Effect of $P_b$ on $\gamma$ diversity
$\sigma_h$	0.012*** (0.003)	0.007*** (0.002)	0.019*** (0.002)
$\sigma_l$	0.060*** (0.003)	-0.047*** (0.002)	0.013*** (0.002)
$\sigma_z$	-0.004 (0.003)	-0.002 (0.002)	-0.006*** (0.002)
$\phi$	0.002 (0.003)	0.001 (0.002)	0.002 (0.002)
$\nu$	-0.001 (0.003)	0.001 (0.002)	-0.001 (0.002)
$\alpha_{max}$	-0.006* (0.003)	-0.001 (0.002)	-0.006*** (0.002)
$\theta$	0.027*** (0.003)	-0.028*** (0.002)	-0.001 (0.002)
$p_d$	0.007** (0.003)	-0.007*** (0.002)	-0.0002 (0.002)
Intercept	0.145*** (0.003)	-0.132*** (0.002)	0.013*** (0.002)
$R^2$	0.522	0.651	0.241

*Note:*

\*p<0.1; \*\*p<0.05; \*\*\*p<0.01



## Table S5 List of fish species in Hokkaido, Japan

**Table S5** List of fish species in Hokkaido, Japan, included in our statistical analysis. 52 species are ordered alphabetically, along with the number of sites present and % occupancy out of 2592 sites.

Species	Number of sites present	Occupancy (%)
<i>Acanthogobius lactipes</i>	63	2.43
<i>Anguilla japonica</i>	1	0.04
<i>Carassius buergeri</i> subsp. 2	4	0.15
<i>Carassius cuvieri</i>	24	0.93
<i>Carassius</i> sp.	213	8.22
<i>Channa argus</i>	3	0.12
<i>Cottus amblystomopsis</i>	48	1.85
<i>Cottus hangiongensis</i>	94	3.63
<i>Cottus nozawae</i>	833	32.14
<i>Cottus</i> sp. ME	25	0.96
<i>Cyprinus carpio</i>	50	1.93
<i>Gasterosteus aculeatus</i>	147	5.67
<i>Gnathopogon caerulescens</i>	1	0.04
<i>Gnathopogon elongatus elongatus</i>	2	0.08
<i>Gymnogobius breunigii</i>	29	1.12
<i>Gymnogobius castaneus</i> complex	145	5.59
<i>Gymnogobius opperiens</i>	85	3.28
<i>Gymnogobius petschiliensis</i>	2	0.08
<i>Gymnogobius urotaenia</i>	290	11.19
<i>Hucho perryi</i>	61	2.35
<i>Hypomesus nipponensis</i>	170	6.56
<i>Hypomesus olidus</i>	8	0.31
<i>Lefua nikkonis</i>	20	0.77
<i>Lethenteron</i> spp.	731	28.20
<i>Leucopsarion petersii</i>	3	0.12
<i>Luciogobius guttatus</i>	3	0.12
<i>Misgurnus anguillicaudatus</i>	212	8.18
<i>Noemacheilus barbatulus</i>	1590	61.34
<i>Oncorhynchus gorbuscha</i>	27	1.04
<i>Oncorhynchus keta</i>	150	5.79
<i>Oncorhynchus masou masou</i>	1417	54.67
<i>Oncorhynchus mykiss</i>	462	17.82
<i>Oncorhynchus nerka</i>	6	0.23
<i>Opsariichthys platypus</i>	1	0.04
<i>Osmerus dentex</i>	7	0.27
<i>Phoxinus phoxinus sachalinensis</i>	68	2.62
<i>Plecoglossus altivelis altivelis</i>	111	4.28
<i>Pseudorasbora parva</i>	94	3.63
<i>Pungitius</i> spp.	285	11.00
<i>Rhinogobius</i> spp.	175	6.75
<i>Rhodeus ocellatus ocellatus</i>	22	0.85
<i>Salangichthys microdon</i>	11	0.42
<i>Salmo trutta</i>	15	0.58
<i>Salvelinus fontinalis</i>	2	0.08
<i>Salvelinus leucomaenis leucomaenis</i>	625	24.11
<i>Salvelinus malma</i>	274	10.57
<i>Salvelinus malma miyabei</i>	2	0.08
<i>Silurus asotus</i>	7	0.27

Species	Number of sites present	Occupancy (%)
<i>Spirinchus lanceolatus</i>	7	0.27
<i>Tribolodon</i> spp.	1163	44.87
<i>Tridentiger brevispinis</i>	135	5.21
<i>Tridentiger obscurus</i>	7	0.27

## Table S6 List of fish species in Midwest, US

**Table S6** List of fish species in the Midwest, US, included in our statistical analysis. 159 species are ordered alphabetically, along with the number of sites present and % occupancy out of 3998 sites.

Species	Number of sites present	Occupancy (%)
<i>Acipenser fulvescens</i>	7	0.18
<i>Alosa pseudoharengus</i>	1	0.03
<i>Ambloplites rupestris</i>	707	17.68
<i>Ameiurus melas</i>	868	21.71
<i>Ameiurus natalis</i>	665	16.63
<i>Ameiurus nebulosus</i>	30	0.75
<i>Amia calva</i>	95	2.38
<i>Ammocrypta clara</i>	12	0.30
<i>Aphredoderus sayanus</i>	76	1.90
<i>Aplodinotus grunniens</i>	208	5.20
<i>Campostoma anomalum</i>	1347	33.69
<i>Campostoma oligolepis</i>	125	3.13
<i>Carpionodes carpio</i>	128	3.20
<i>Carpionodes cyprinus</i>	234	5.85
<i>Carpionodes velifer</i>	82	2.05
<i>Catostomus commersonii</i>	2931	73.31
<i>Centrarchus macropterus</i>	5	0.13
<i>Chrosomus eos</i>	336	8.40
<i>Chrosomus neogaeus</i>	103	2.58
<i>Clinostomus elongatus</i>	97	2.43
<i>Cottus bairdii</i>	467	11.68
<i>Cottus carolinae</i>	6	0.15
<i>Cottus cognatus</i>	38	0.95
<i>Crystallaria asprella</i>	1	0.03
<i>Ctenopharyngodon idella</i>	19	0.48
<i>Culaea inconstans</i>	1531	38.29
<i>Cyprinella lutrensis</i>	269	6.73
<i>Cyprinella spiloptera</i>	780	19.51
<i>Cyprinella venusta</i>	2	0.05
<i>Cyprinella whipplei</i>	33	0.83
<i>Cyprinus carpio</i>	946	23.66
<i>Dorosoma cepedianum</i>	208	5.20
<i>Erimystax x-punctatus</i>	13	0.33
<i>Erimyzon oblongus</i>	63	1.58
<i>Erimyzon sucetta</i>	10	0.25
<i>Esox americanus vermiculatus</i>	117	2.93
<i>Esox lucius</i>	957	23.94
<i>Esox masquinongy</i>	20	0.50
<i>Etheostoma asprigene</i>	10	0.25
<i>Etheostoma blennioides</i>	1	0.03
<i>Etheostoma caeruleum</i>	195	4.88
<i>Etheostoma chlorosomum</i>	4	0.10
<i>Etheostoma crossopterus</i>	4	0.10
<i>Etheostoma exile</i>	261	6.53
<i>Etheostoma flabellare</i>	843	21.09
<i>Etheostoma gracile</i>	15	0.38
<i>Etheostoma kennicotti</i>	1	0.03
<i>Etheostoma microperca</i>	20	0.50

Species	Number of sites present	Occupancy (%)
<i>Etheostoma nigrum</i>	2546	63.68
<i>Etheostoma proeliare</i>	2	0.05
<i>Etheostoma spectabile</i>	121	3.03
<i>Etheostoma squamiceps</i>	4	0.10
<i>Etheostoma zonale</i>	321	8.03
<i>Fundulus diaphanus</i>	3	0.08
<i>Fundulus dispar</i>	4	0.10
<i>Fundulus notatus</i>	282	7.05
<i>Fundulus olivaceus</i>	42	1.05
<i>Hiodon alosoides</i>	3	0.08
<i>Hiodon tergisus</i>	16	0.40
<i>Hybognathus hankinsoni</i>	576	14.41
<i>Hybognathus nuchalis</i>	24	0.60
<i>Hybopsis amnis</i>	1	0.03
<i>Hypentelium nigricans</i>	682	17.06
<i>Hypophthalmichthys molitrix</i>	14	0.35
<i>Hypophthalmichthys nobilis</i>	3	0.08
<i>Ichthyomyzon castaneus</i>	51	1.28
<i>Ichthyomyzon fossor</i>	35	0.88
<i>Ichthyomyzon gagei</i>	6	0.15
<i>Ichthyomyzon unicuspis</i>	9	0.23
<i>Ictalurus punctatus</i>	413	10.33
<i>Ictiobus bubalus</i>	90	2.25
<i>Ictiobus cyprinellus</i>	129	3.23
<i>Ictiobus niger</i>	41	1.03
<i>Labidesthes sicculus</i>	64	1.60
<i>Lepisosteus oculatus</i>	13	0.33
<i>Lepisosteus osseus</i>	25	0.63
<i>Lepisosteus platostomus</i>	58	1.45
<i>Lepomis cyanellus</i>	1575	39.39
<i>Lepomis gibbosus</i>	290	7.25
<i>Lepomis gulosus</i>	43	1.08
<i>Lepomis humilis</i>	356	8.90
<i>Lepomis macrochirus</i>	1051	26.29
<i>Lepomis megalotis</i>	186	4.65
<i>Lepomis microlophus</i>	19	0.48
<i>Lethenteron appendix</i>	122	3.05
<i>Lota lota</i>	266	6.65
<i>Luxilus chrysocephalus</i>	198	4.95
<i>Luxilus cornutus</i>	1784	44.62
<i>Lythrurus fumeus</i>	6	0.15
<i>Lythrurus umbratilis</i>	224	5.60
<i>Macrhybopsis aestivalis</i>	1	0.03
<i>Macrhybopsis hyostoma</i>	3	0.08
<i>Macrhybopsis storeriana</i>	10	0.25
<i>Micropterus dolomieu</i>	748	18.71
<i>Micropterus punctulatus</i>	15	0.38
<i>Micropterus salmoides</i>	987	24.69
<i>Minytrema melanops</i>	41	1.03
<i>Morone americana</i>	2	0.05
<i>Morone chrysops</i>	65	1.63
<i>Morone mississippiensis</i>	16	0.40

Species	Number of sites present	Occupancy (%)
Moxostoma anisurum	288	7.20
Moxostoma carinatum	8	0.20
Moxostoma duquesni	103	2.58
Moxostoma erythrurum	709	17.73
Moxostoma macrolepidotum	737	18.43
Moxostoma valenciennesi	85	2.13
Neogobius melanostomus	13	0.33
Nocomis biguttatus	1287	32.19
Notemigonus crysoleucas	377	9.43
Notropis anogenus	10	0.25
Notropis atherinoides	207	5.18
Notropis blennius	16	0.40
Notropis boops	9	0.23
Notropis buccatus	47	1.18
Notropis chalybaeus	11	0.28
Notropis dorsalis	1088	27.21
Notropis heterodon	28	0.70
Notropis heterolepis	187	4.68
Notropis hudsonius	81	2.03
Notropis nubilus	58	1.45
Notropis percobromus	167	4.18
Notropis rubellus	63	1.58
Notropis stramineus	975	24.39
Notropis texanus	20	0.50
Notropis volucellus	81	2.03
Notropis wickliffi	10	0.25
Noturus exilis	34	0.85
Noturus flavus	479	11.98
Noturus gyrinus	447	11.18
Noturus nocturnus	38	0.95
Oncorhynchus mykiss	55	1.38
Oncorhynchus tshawytscha	1	0.03
Opsopoeodus emiliae	3	0.08
Perca flavescens	622	15.56
Percina caprodes	337	8.43
Percina carprodes semifasciata	7	0.18
Percina evides	16	0.40
Percina maculata	888	22.21
Percina phoxocephala	259	6.48
Percina sciera	2	0.05
Percopsis omiscomaycus	21	0.53
Phenacobius mirabilis	259	6.48
Phoxinus erythrogaster	417	10.43
Pimephales notatus	1784	44.62
Pimephales promelas	1535	38.39
Pimephales vigilax	84	2.10
Pomoxis annularis	61	1.53
Pomoxis nigromaculatus	376	9.40
Pylodictis olivaris	73	1.83
Rhinichthys atratulus	1120	28.01
Rhinichthys cataractae	627	15.68
Rhinichthys obtusus	449	11.23

Species	Number of sites present	Occupancy (%)
<i>Salmo trutta</i>	399	9.98
<i>Salvelinus fontinalis</i>	369	9.23
<i>Sander canadensis</i>	39	0.98
<i>Sander vitreus</i>	367	9.18
<i>Scaphirhynchus platyrhynchus</i>	8	0.20
<i>Semotilus atromaculatus</i>	2776	69.43
<i>Umbra limi</i>	1600	40.02

## Figures

**Figure S1** Longitudinal gradient of local species richness ( $\sigma_h = 1$ ,  $\sigma_l = 0.01$ )

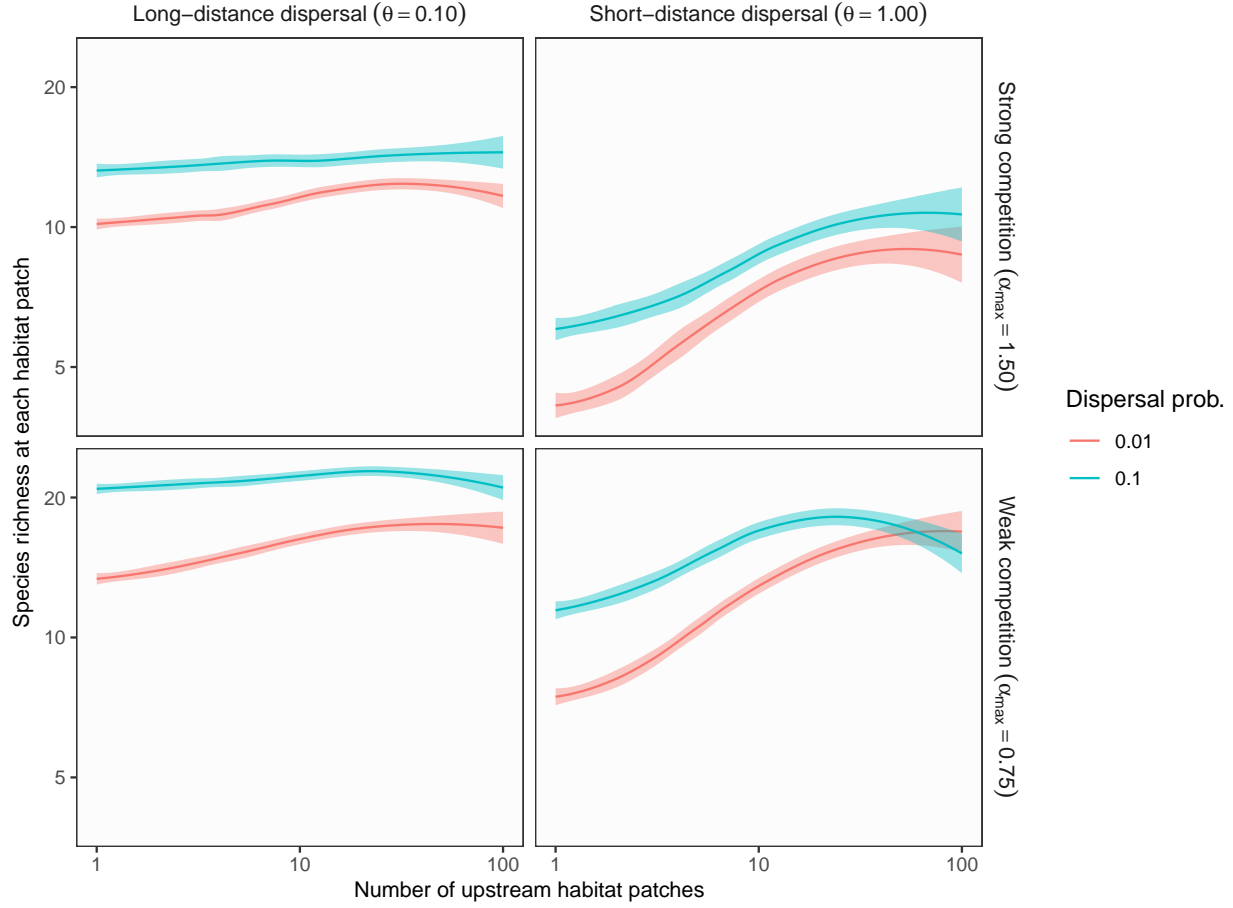


**Figure S1** Theoretical predictions for longitudinal gradients of local species richness in branching networks. The longitudinal position of each habitat patch (x axis) was expressed as the number of upstream contributing patches. In this simulation, environmental variation at headwaters ( $\sigma_h$ ) exceeds local environmental noise ( $\sigma_l$ ). Lines and shades are loess curves fitted to simulated data and their 95% confidence intervals. Each panel represents different ecological scenarios under which metacommunity dynamics were simulated. Rows represent different competition strength. Competitive coefficients ( $\alpha_{ij}$ ) were varied randomly from 0 to 1.5 (top, strong competition) or 0.75 (bottom, weak competition). Columns and lines represent different dispersal scenarios (dispersal distance and probability). Left and right columns show long-distance (the rate parameter of an exponential dispersal kernel  $\theta = 0.10$ ) and short-distance dispersal ( $\theta = 1.0$ ) scenarios respectively. Red and blue lines show low ( $p_d = 0.01$ ) and high dispersal probabilities ( $p_d = 0.10$ ). Other parameters are as follows: environmental variation at headwaters  $\sigma_h = 1$ ; local environmental noise  $\sigma_l = 0.01$ ; ecosystem size  $N_p = 100$ ; ecosystem complexity  $P_b = 0.5$ .

**Figure S2** Longitudinal gradient of local species richness ( $\sigma_h = 1$ ,  $\sigma_l = 1$ )

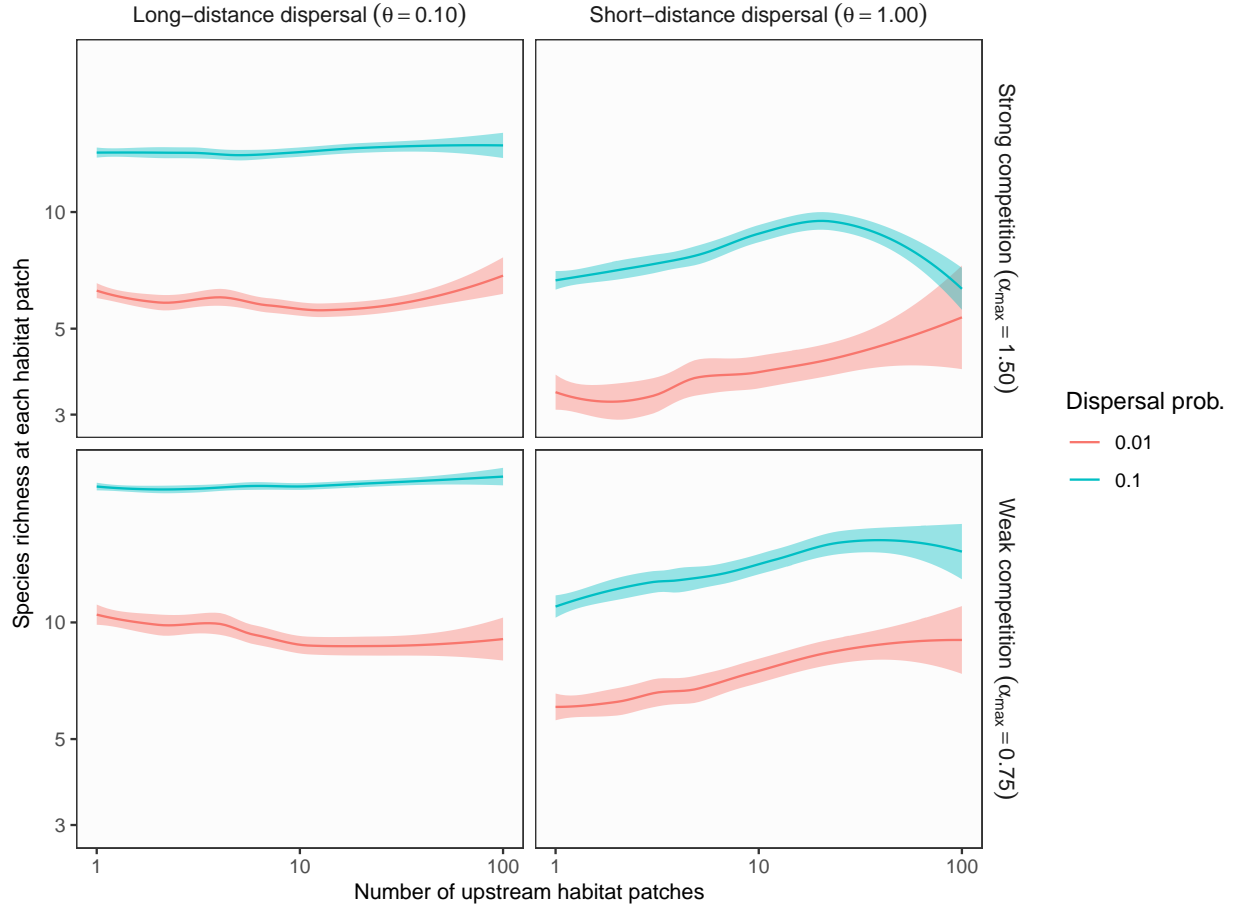


**Figure S2** Theoretical predictions for longitudinal gradients of local species richness in branching networks. The longitudinal position of each habitat patch (x axis) was expressed as the number of upstream contributing patches. In this simulation, environmental variation at headwaters ( $\sigma_h$ ) is equal to local environmental noise ( $\sigma_l$ ). Lines and shades are loess curves fitted to simulated data and their 95% confidence intervals. Each panel represents different ecological scenarios under which metacommunity dynamics were simulated. Rows represent different competition strength. Competitive coefficients ( $\alpha_{ij}$ ) were varied randomly from 0 to 1.5 (top, strong competition) or 0.75 (bottom, weak competition). Columns and lines represent different dispersal scenarios (dispersal distance and probability). Left and right columns show long-distance (the rate parameter of an exponential dispersal kernel  $\theta = 0.10$ ) and short-distance dispersal ( $\theta = 1.0$ ) scenarios respectively. Red and blue lines show low ( $p_d = 0.01$ ) and high dispersal probabilities ( $p_d = 0.10$ ). Other parameters are as follows: environmental variation at headwaters  $\sigma_h = 1$ ; local environmental noise  $\sigma_l = 1$ ; ecosystem size  $N_p = 100$ ; ecosystem complexity  $P_b = 0.5$ .



**Figure S3 Longitudinal gradient of local species richness ( $\sigma_h = 0.01$ ,  $\sigma_l = 0.01$ )**

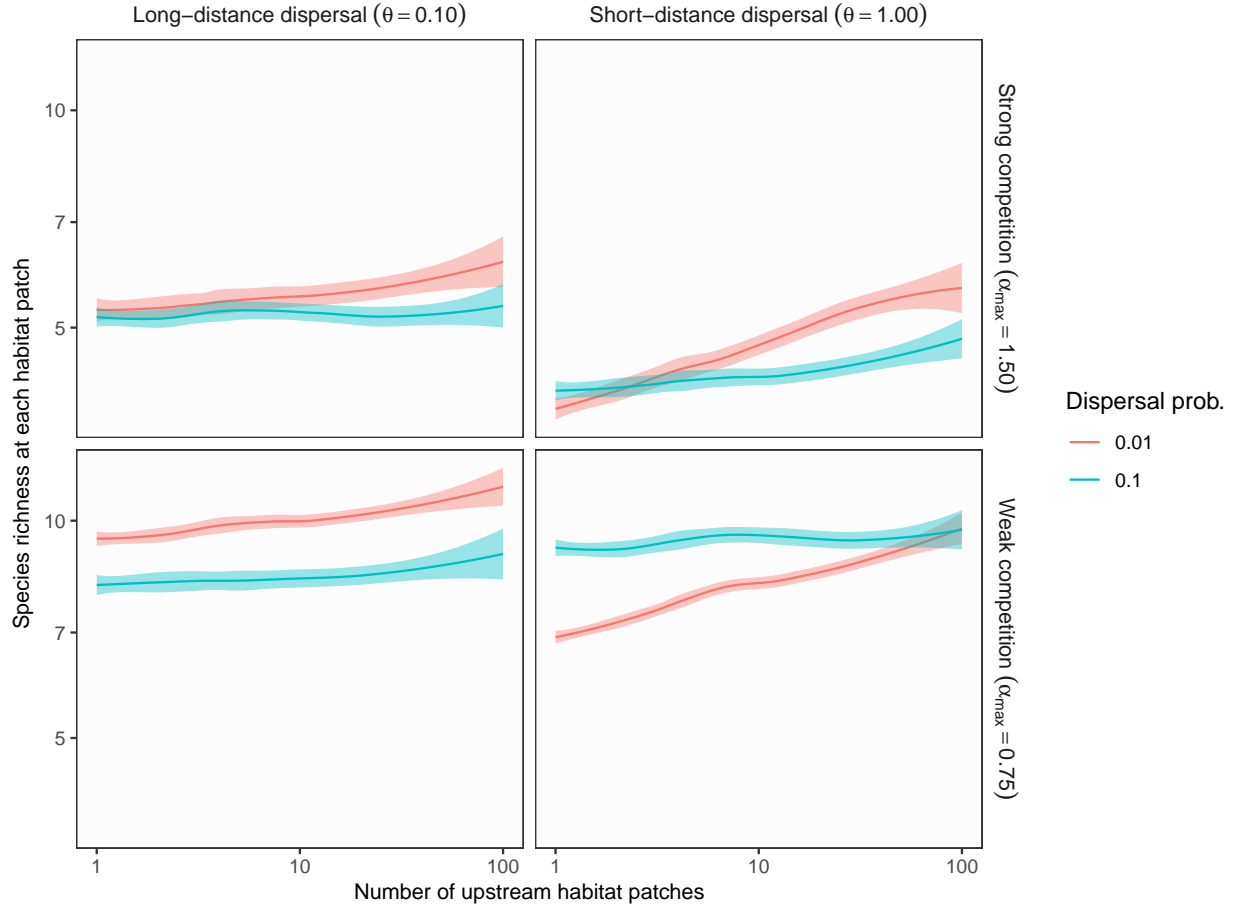


**Figure S3** Theoretical predictions for longitudinal gradients of local species richness in branching networks. The longitudinal position of each habitat patch (x axis) was expressed as the number of upstream contributing patches. In this simulation, environmental variation at headwaters ( $\sigma_h$ ) is equal to local environmental noise ( $\sigma_l$ ). Lines and shades are loess curves fitted to simulated data and their 95% confidence intervals. Each panel represents different ecological scenarios under which metacommunity dynamics were simulated. Rows represent different competition strength. Competitive coefficients ( $\alpha_{ij}$ ) were varied randomly from 0 to 1.5 (top, strong competition) or 0.75 (bottom, weak competition). Columns and lines represent different dispersal scenarios (dispersal distance and probability). Left and right columns show long-distance (the rate parameter of an exponential dispersal kernel  $\theta = 0.10$ ) and short-distance dispersal ( $\theta = 1.0$ ) scenarios respectively. Red and blue lines show low ( $p_d = 0.01$ ) and high dispersal probabilities ( $p_d = 0.10$ ). Other parameters are as follows: environmental variation at headwaters  $\sigma_h = 0.01$ ; local environmental noise  $\sigma_l = 0.01$ ; ecosystem size  $N_p = 100$ ; ecosystem complexity  $P_b = 0.5$ .

**Figure S4 Longitudinal gradient of local species richness ( $\sigma_h = 0.01$ ,  $\sigma_l = 1$ )**

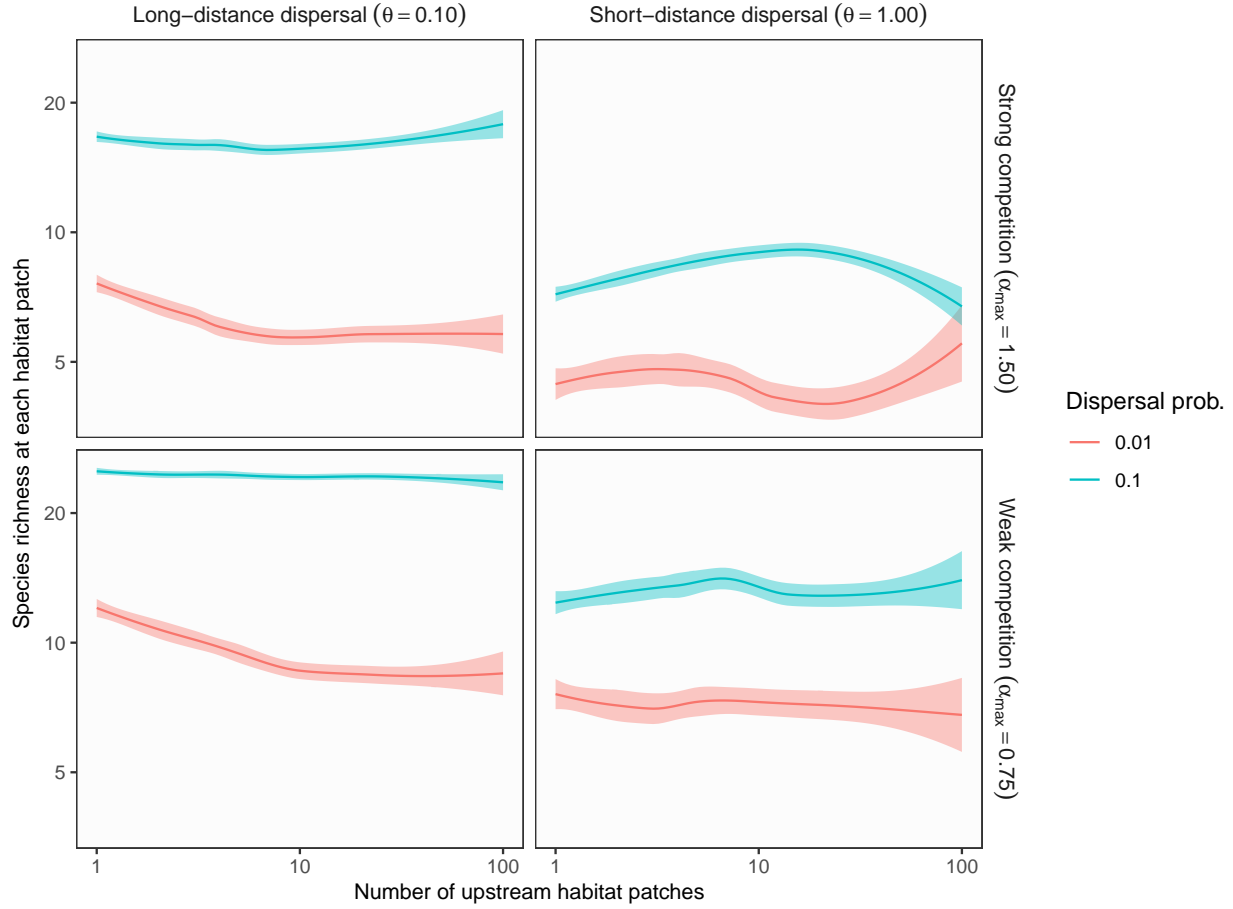


**Figure S4** Theoretical predictions for longitudinal gradients of local species richness in branching networks. The longitudinal position of each habitat patch (x axis) was expressed as the number of upstream contributing patches. In this simulation, environmental variation at headwaters ( $\sigma_h$ ) is less than local environmental noise ( $\sigma_l$ ). Lines and shades are loess curves fitted to simulated data and their 95% confidence intervals. Each panel represents different ecological scenarios under which metacommunity dynamics were simulated. Rows represent different competition strength. Competitive coefficients ( $\alpha_{ij}$ ) were varied randomly from 0 to 1.5 (top, strong competition) or 0.75 (bottom, weak competition). Columns and lines represent different dispersal scenarios (dispersal distance and probability). Left and right columns show long-distance (the rate parameter of an exponential dispersal kernel  $\theta = 0.10$ ) and short-distance dispersal ( $\theta = 1.0$ ) scenarios respectively. Red and blue lines show low ( $p_d = 0.01$ ) and high dispersal probabilities ( $p_d = 0.10$ ). Other parameters are as follows: environmental variation at headwaters  $\sigma_h = 0.01$ ; local environmental noise  $\sigma_l = 1$ ; ecosystem size  $N_p = 100$ ; ecosystem complexity  $P_b = 0.5$ .

**Figure S5 Influence of ecosystem size ( $p_d = 0.1$ ,  $\sigma_h = 1$ ,  $\sigma_l = 0.01$ )**

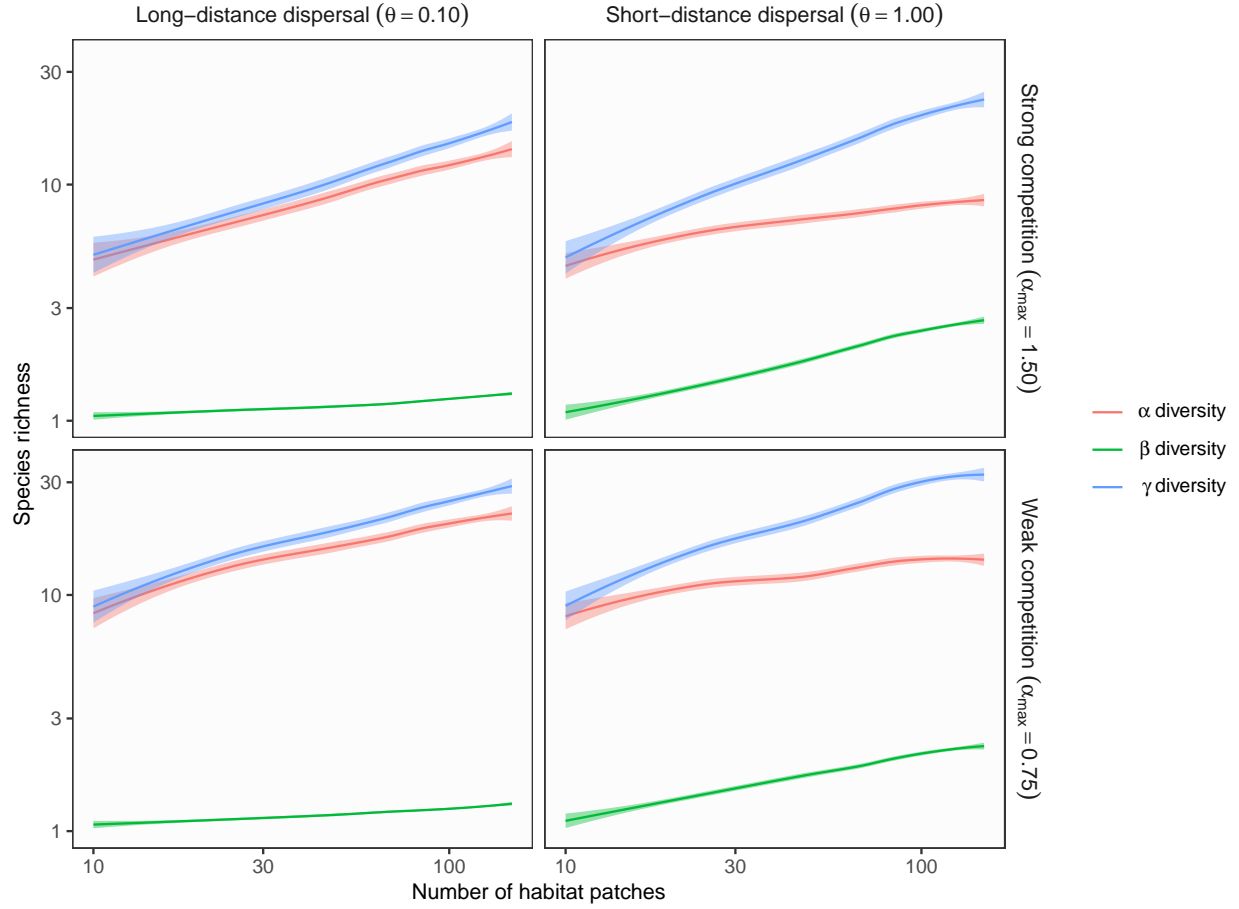


**Figure S5** Theoretical predictions for ecosystem size influences (the number of habitat patches) on  $\alpha$ ,  $\beta$ , and  $\gamma$  diversity in branching networks. In this simulation, environmental variation at headwaters ( $\sigma_h$ ) exceeds local environmental noise ( $\sigma_l$ ). Lines and shades are loess curves fitted to simulated data and their 95% confidence intervals. Each panel represents different ecological scenarios under which metacommunity dynamics were simulated. Rows represent different competition strength. Competitive coefficients ( $\alpha_{ij}$ ) were varied randomly from 0 to 1.5 (top, strong competition) or 0.75 (bottom, weak competition). Columns represent different dispersal scenarios. Two dispersal parameters were chosen to simulate scenarios with long-distance (the rate parameter of an exponential dispersal kernel  $\theta = 0.10$ ) and short-distance dispersal ( $\theta = 1.0$ ). Other parameters are as follows: dispersal probability  $p_d = 0.1$ ; environmental variation at headwaters  $\sigma_h = 1$ ; local environmental noise  $\sigma_l = 0.01$ .

**Figure S6 Influence of ecosystem size ( $p_d = 0.1$ ,  $\sigma_h = 1$ ,  $\sigma_l = 1$ )**

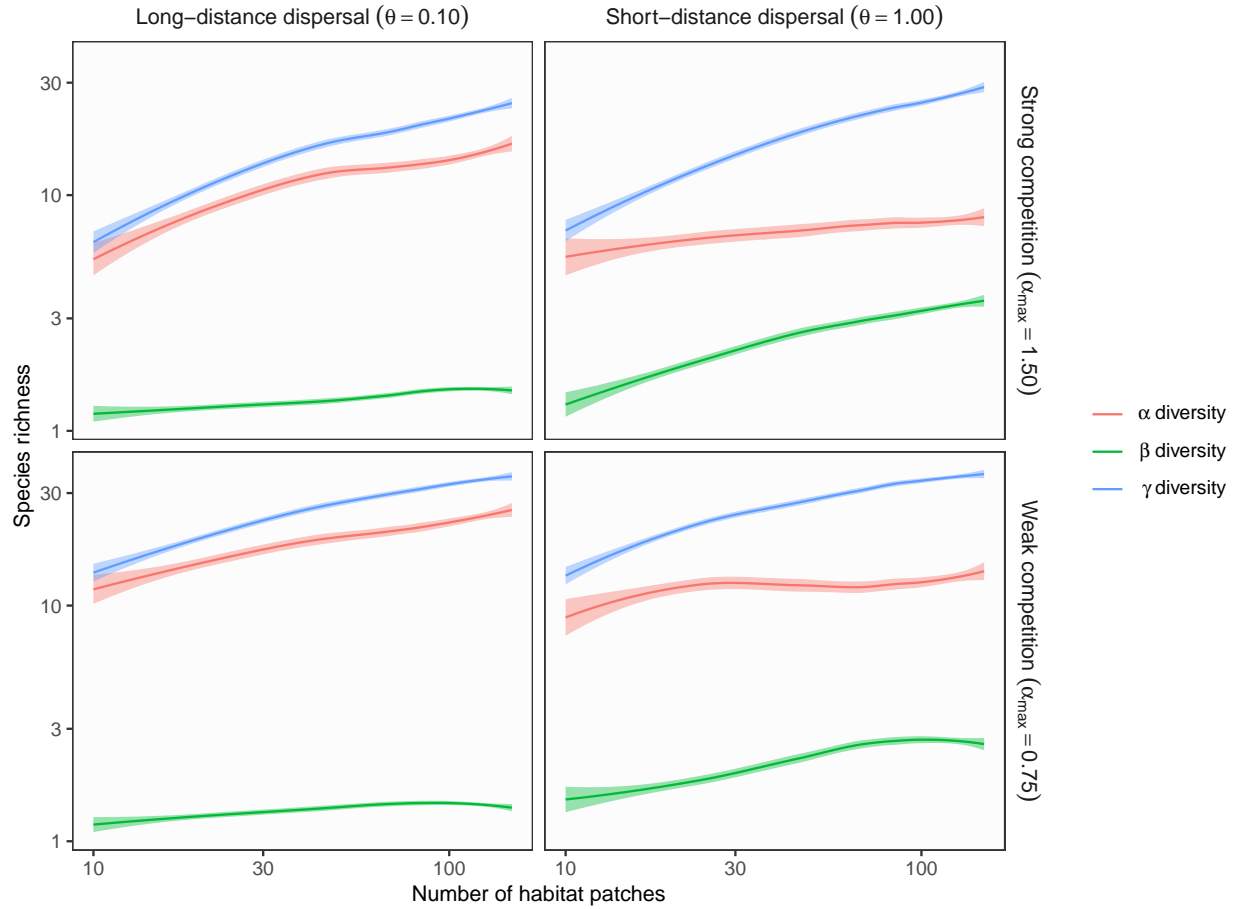


**Figure S6** Theoretical predictions for ecosystem size influences (the number of habitat patches) on  $\alpha$ ,  $\beta$ , and  $\gamma$  diversity in branching networks. In this simulation, environmental variation at headwaters ( $\sigma_h$ ) is equal to local environmental noise ( $\sigma_l$ ). Lines and shades are loess curves fitted to simulated data and their 95% confidence intervals. Each panel represents different ecological scenarios under which metacommunity dynamics were simulated. Rows represent different competition strength. Competitive coefficients ( $\alpha_{ij}$ ) were varied randomly from 0 to 1.5 (top, strong competition) or 0.75 (bottom, weak competition). Columns represent different dispersal scenarios. Two dispersal parameters were chosen to simulate scenarios with long-distance (the rate parameter of an exponential dispersal kernel  $\theta = 0.10$ ) and short-distance dispersal ( $\theta = 1.0$ ). Other parameters are as follows: dispersal probability  $p_d = 0.1$ ; environmental variation at headwaters  $\sigma_h = 1$ ; local environmental noise  $\sigma_l = 1$ .

**Figure S7 Influence of ecosystem size ( $p_d = 0.1$ ,  $\sigma_h = 0.01$ ,  $\sigma_l = 0.01$ )**

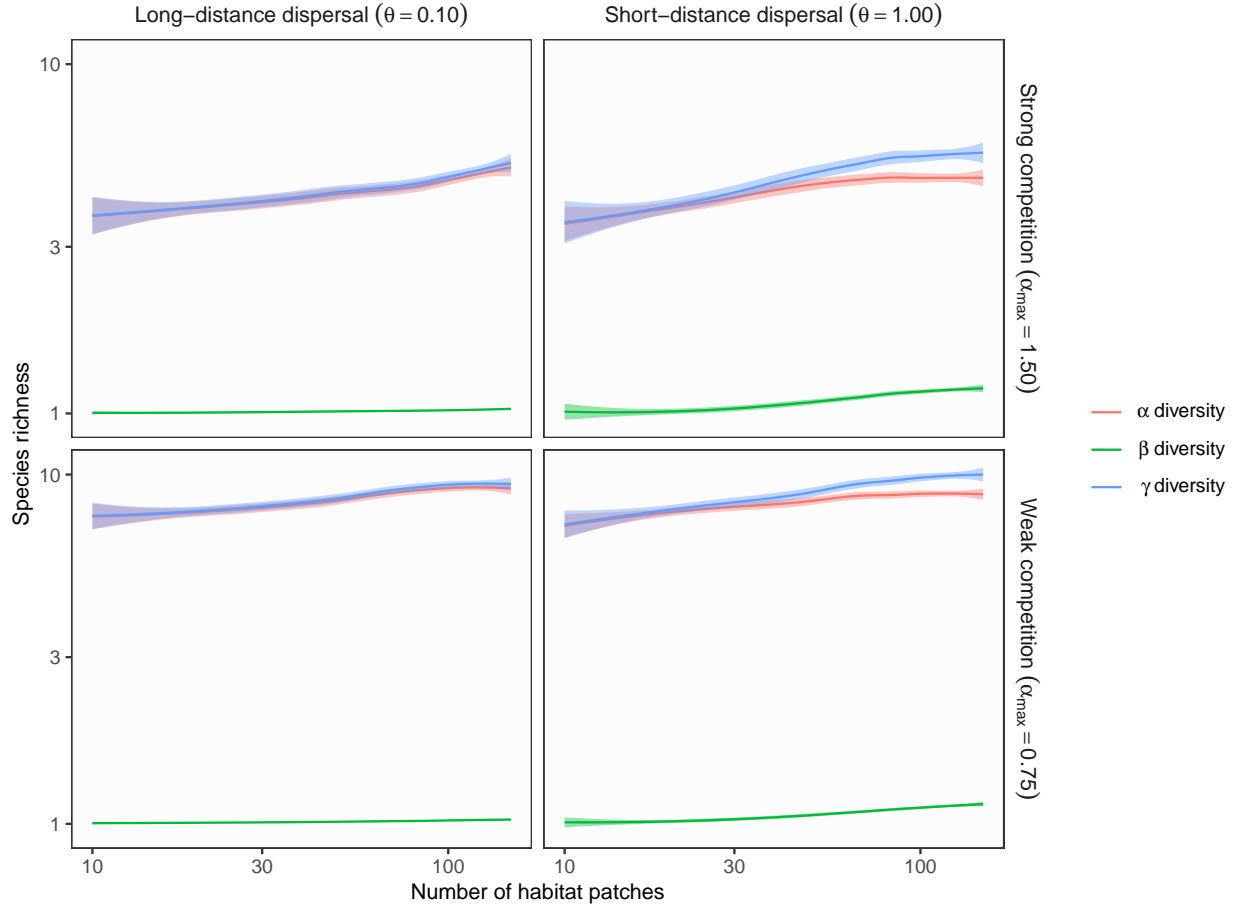


**Figure S7** Theoretical predictions for ecosystem size influences (the number of habitat patches) on  $\alpha$ ,  $\beta$ , and  $\gamma$  diversity in branching networks. In this simulation, environmental variation at headwaters ( $\sigma_h$ ) is equal to local environmental noise ( $\sigma_l$ ). Lines and shades are loess curves fitted to simulated data and their 95% confidence intervals. Each panel represents different ecological scenarios under which metacommunity dynamics were simulated. Rows represent different competition strength. Competitive coefficients ( $\alpha_{ij}$ ) were varied randomly from 0 to 1.5 (top, strong competition) or 0.75 (bottom, weak competition). Columns represent different dispersal scenarios. Two dispersal parameters were chosen to simulate scenarios with long-distance (the rate parameter of an exponential dispersal kernel  $\theta = 0.10$ ) and short-distance dispersal ( $\theta = 1.0$ ). Other parameters are as follows: dispersal probability  $p_d = 0.1$ ; environmental variation at headwaters  $\sigma_h = 0.01$ ; local environmental noise  $\sigma_l = 0.01$ .

**Figure S8 Influence of ecosystem size ( $p_d = 0.1$ ,  $\sigma_h = 0.01$ ,  $\sigma_l = 1$ )**

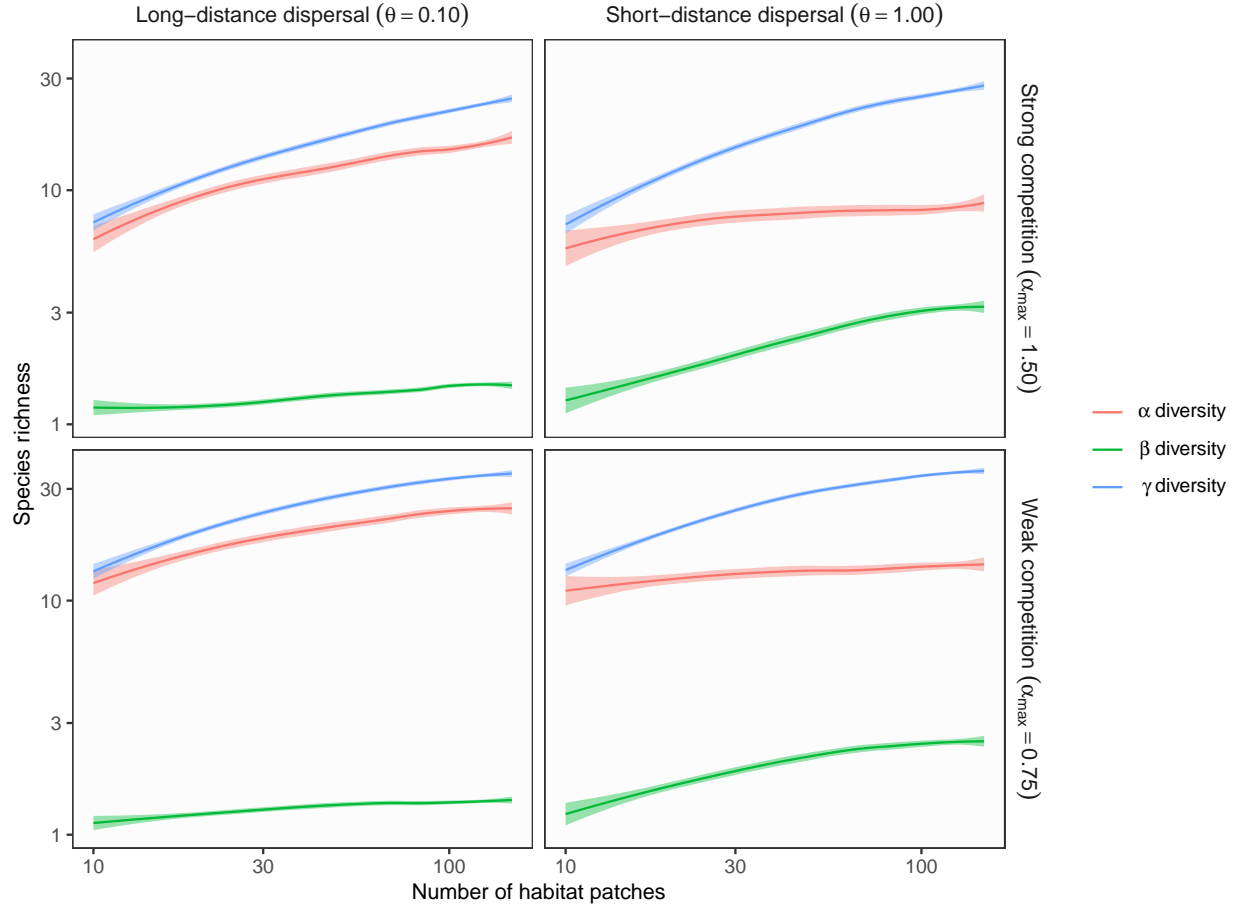


**Figure S8** Theoretical predictions for ecosystem size influences (the number of habitat patches) on  $\alpha$ ,  $\beta$ , and  $\gamma$  diversity in branching networks. In this simulation, environmental variation at headwaters ( $\sigma_h$ ) is less than local environmental noise ( $\sigma_l$ ). Lines and shades are loess curves fitted to simulated data and their 95% confidence intervals. Each panel represents different ecological scenarios under which metacommunity dynamics were simulated. Rows represent different competition strength. Competitive coefficients ( $\alpha_{ij}$ ) were varied randomly from 0 to 1.5 (top, strong competition) or 0.75 (bottom, weak competition). Columns represent different dispersal scenarios. Two dispersal parameters were chosen to simulate scenarios with long-distance (the rate parameter of an exponential dispersal kernel  $\theta = 0.10$ ) and short-distance dispersal ( $\theta = 1.0$ ). Other parameters are as follows: dispersal probability  $p_d = 0.1$ ; environmental variation at headwaters  $\sigma_h = 0.01$ ; local environmental noise  $\sigma_l = 1$ .

**Figure S9 Influence of ecosystem size ( $p_d = 0.01$ ,  $\sigma_h = 1$ ,  $\sigma_l = 1$ )**

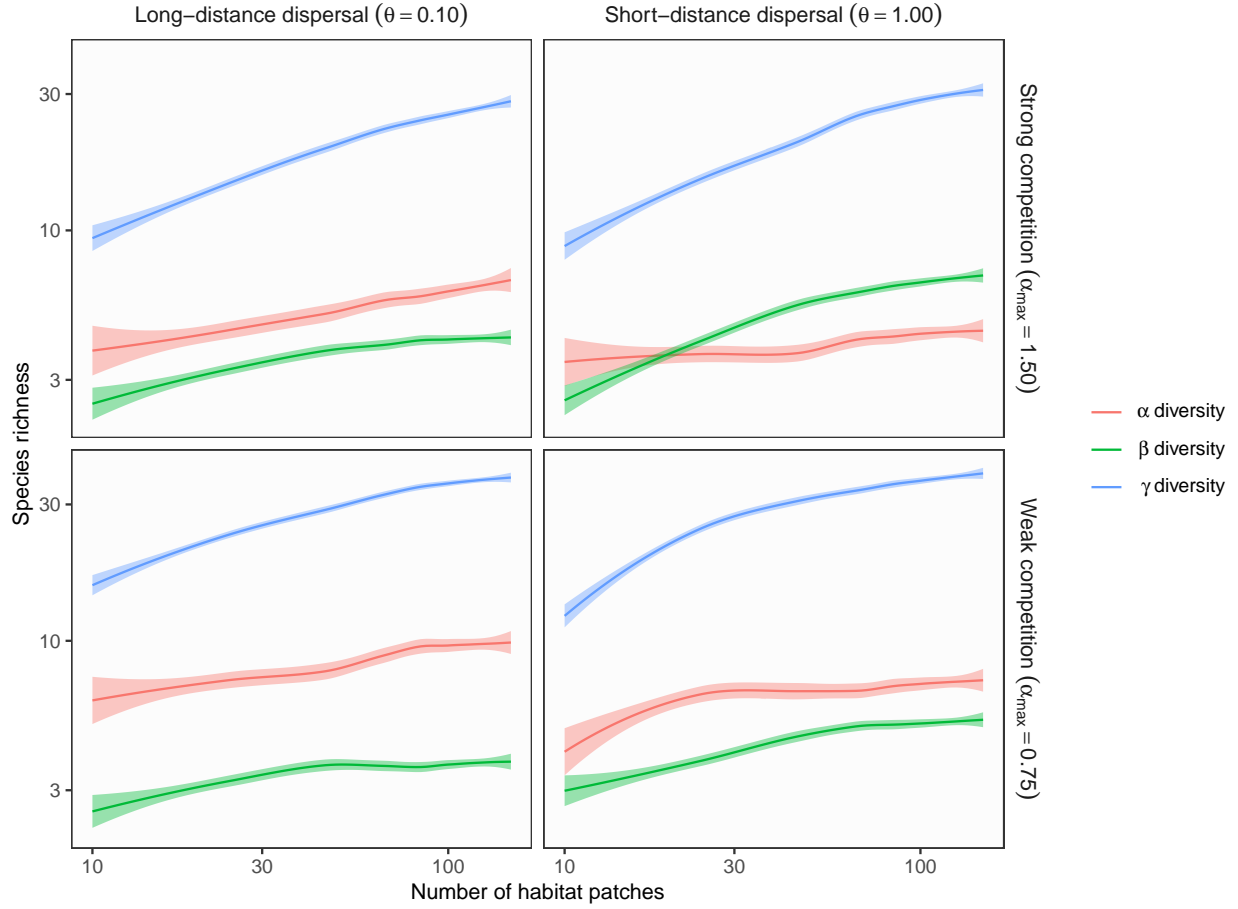


**Figure S9** Theoretical predictions for ecosystem size influences (the number of habitat patches) on  $\alpha$ ,  $\beta$ , and  $\gamma$  diversity in branching networks. In this simulation, environmental variation at headwaters ( $\sigma_h$ ) is equal to local environmental noise ( $\sigma_l$ ). Lines and shades are loess curves fitted to simulated data and their 95% confidence intervals. Each panel represents different ecological scenarios under which metacommunity dynamics were simulated. Rows represent different competition strength. Competitive coefficients ( $\alpha_{ij}$ ) were varied randomly from 0 to 1.5 (top, strong competition) or 0.75 (bottom, weak competition). Columns represent different dispersal scenarios. Two dispersal parameters were chosen to simulate scenarios with long-distance (the rate parameter of an exponential dispersal kernel  $\theta = 0.10$ ) and short-distance dispersal ( $\theta = 1.0$ ). Other parameters are as follows: dispersal probability  $p_d = 0.01$ ; environmental variation at headwaters  $\sigma_h = 1$ ; local environmental noise  $\sigma_l = 1$ .

**Figure S10 Influence of ecosystem size ( $p_d = 0.01$ ,  $\sigma_h = 0.01$ ,  $\sigma_l = 0.01$ )**

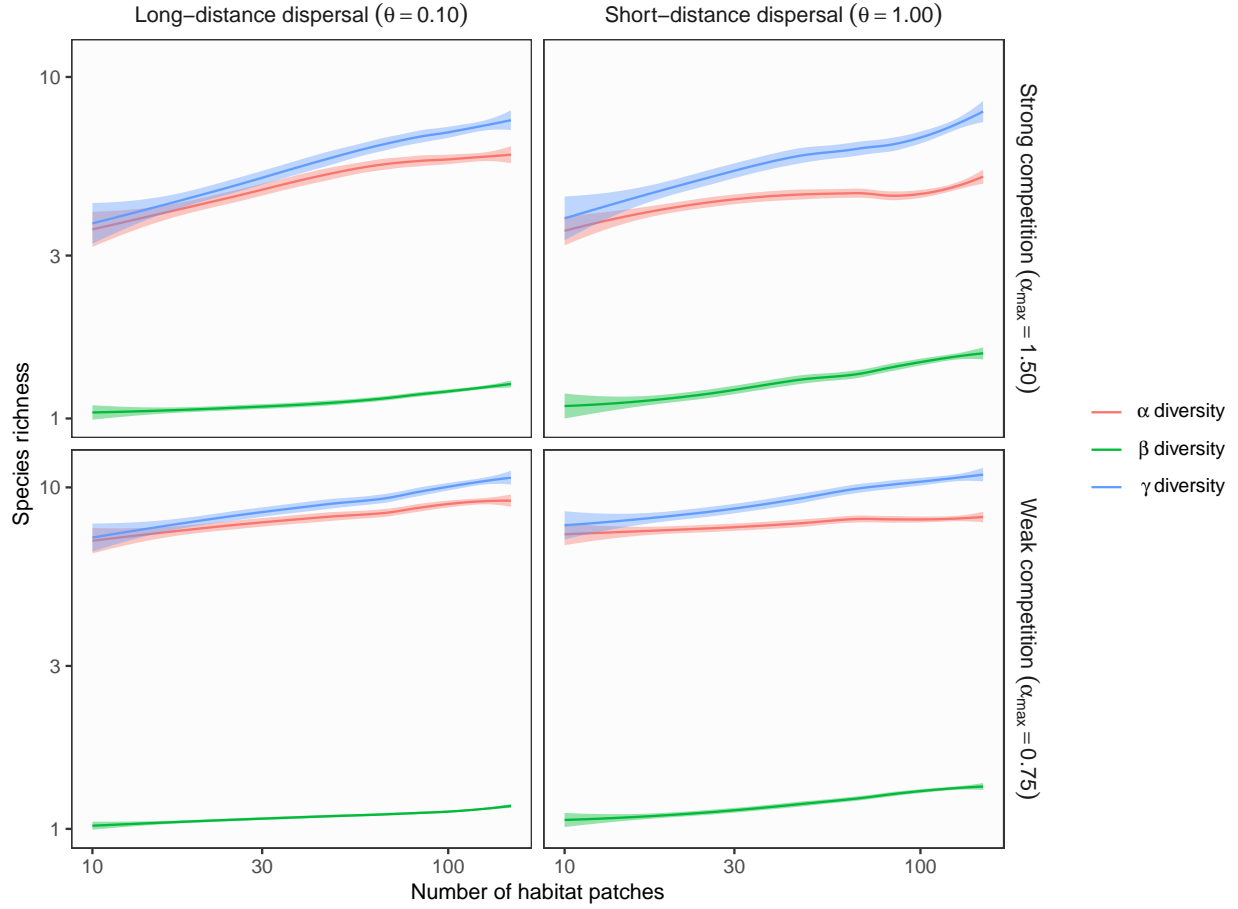


**Figure S10** Theoretical predictions for ecosystem size influences (the number of habitat patches) on  $\alpha$ ,  $\beta$ , and  $\gamma$  diversity in branching networks. In this simulation, environmental variation at headwaters ( $\sigma_h$ ) is equal to local environmental noise ( $\sigma_l$ ). Lines and shades are loess curves fitted to simulated data and their 95% confidence intervals. Each panel represents different ecological scenarios under which metacommunity dynamics were simulated. Rows represent different competition strength. Competitive coefficients ( $\alpha_{ij}$ ) were varied randomly from 0 to 1.5 (top, strong competition) or 0.75 (bottom, weak competition). Columns represent different dispersal scenarios. Two dispersal parameters were chosen to simulate scenarios with long-distance (the rate parameter of an exponential dispersal kernel  $\theta = 0.10$ ) and short-distance dispersal ( $\theta = 1.0$ ). Other parameters are as follows: dispersal probability  $p_d = 0.01$ ; environmental variation at headwaters  $\sigma_h = 0.01$ ; local environmental noise  $\sigma_l = 0.01$ .



**Figure S11 Influence of ecosystem size ( $p_d = 0.01$ ,  $\sigma_h = 0.01$ ,  $\sigma_l = 1$ )**

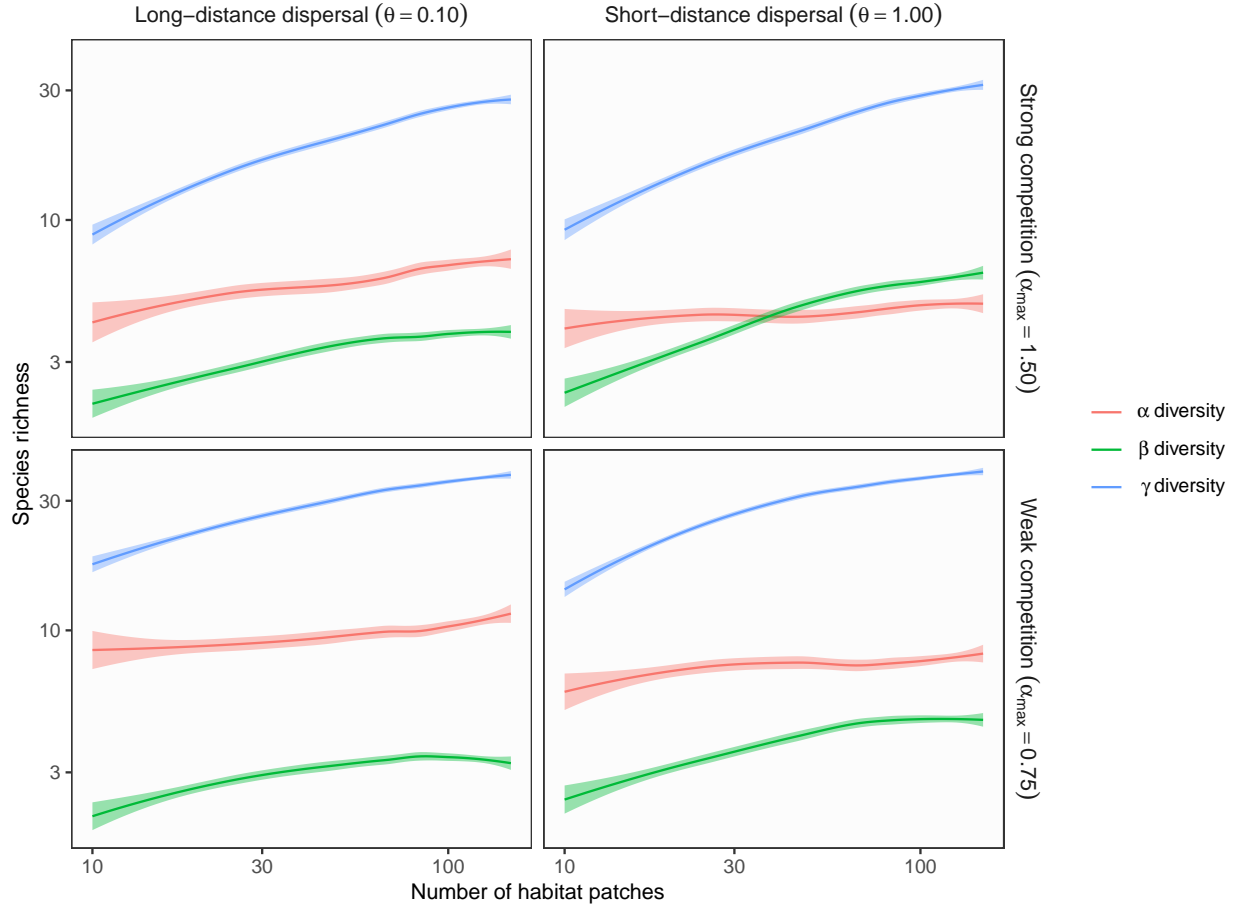


**Figure S11** Theoretical predictions for ecosystem size influences (the number of habitat patches) on  $\alpha$ ,  $\beta$ , and  $\gamma$  diversity in branching networks. In this simulation, environmental variation at headwaters ( $\sigma_h$ ) is less than local environmental noise ( $\sigma_l$ ). Lines and shades are loess curves fitted to simulated data and their 95% confidence intervals. Each panel represents different ecological scenarios under which metacommunity dynamics were simulated. Rows represent different competition strength. Competitive coefficients ( $\alpha_{ij}$ ) were varied randomly from 0 to 1.5 (top, strong competition) or 0.75 (bottom, weak competition). Columns represent different dispersal scenarios. Two dispersal parameters were chosen to simulate scenarios with long-distance (the rate parameter of an exponential dispersal kernel  $\theta = 0.10$ ) and short-distance dispersal ( $\theta = 1.0$ ). Other parameters are as follows: dispersal probability  $p_d = 0.01$ ; environmental variation at headwaters  $\sigma_h = 0.01$ ; local environmental noise  $\sigma_l = 1$ .

**Figure S12 Influence of ecosystem complexity ( $p_d = 0.1$ ,  $\sigma_h = 1$ ,  $\sigma_l = 0.01$ )**

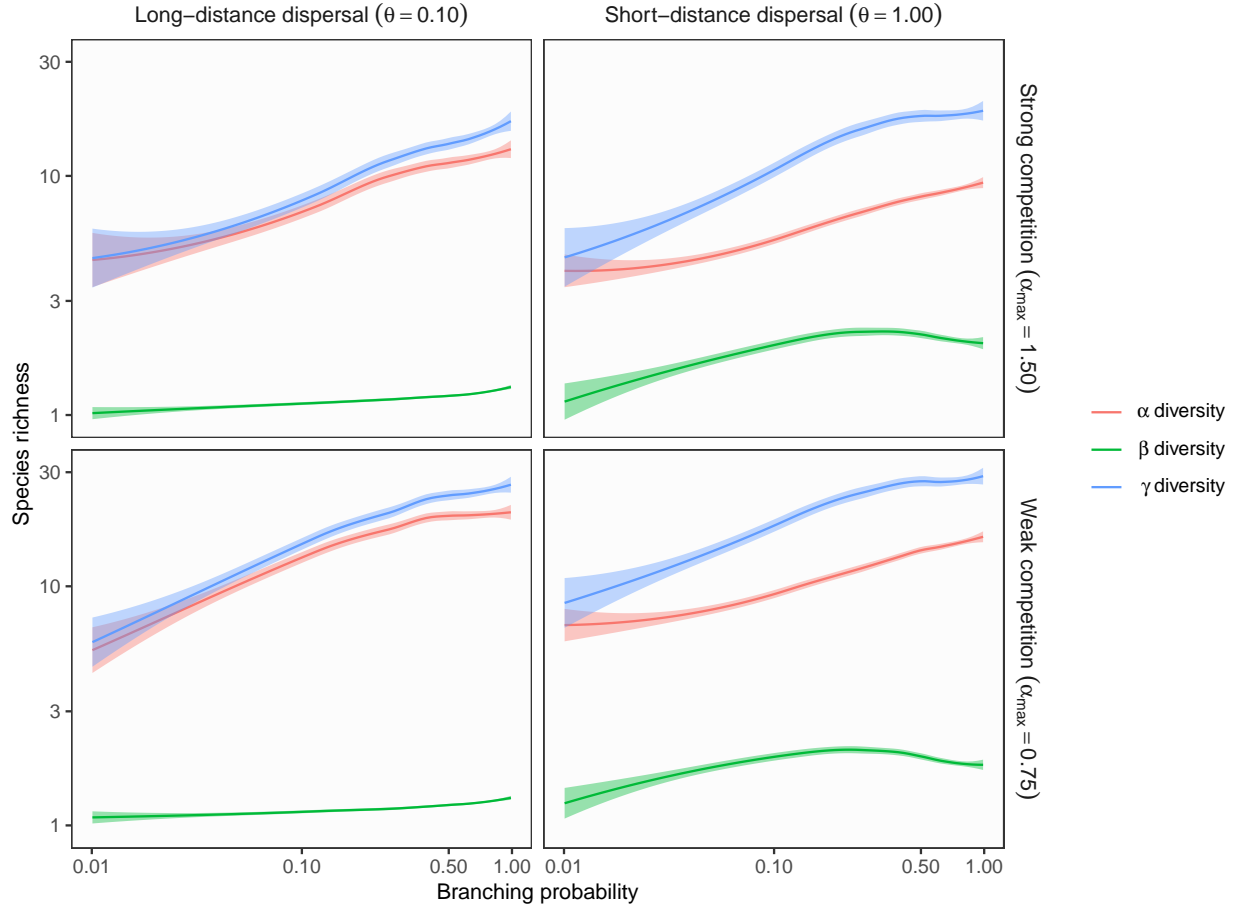


**Figure S12** Theoretical predictions for ecosystem complexity influences (branching probability) on  $\alpha$ ,  $\beta$ , and  $\gamma$  diversity in branching networks. In this simulation, environmental variation at headwaters ( $\sigma_h$ ) exceeds local environmental noise ( $\sigma_l$ ). Lines and shades are loess curves fitted to simulated data and their 95% confidence intervals. Each panel represents different ecological scenarios under which metacommunity dynamics were simulated. Rows represent different competition strength. Competitive coefficients ( $\alpha_{ij}$ ) were varied randomly from 0 to 1.5 (top, strong competition) or 0.75 (bottom, weak competition). Columns represent different dispersal scenarios. Two dispersal parameters were chosen to simulate scenarios with long-distance (the rate parameter of an exponential dispersal kernel  $\theta = 0.10$ ) and short-distance dispersal ( $\theta = 1.0$ ). Other parameters are as follows: dispersal probability  $p_d = 0.1$ ; environmental variation at headwaters  $\sigma_h = 1$ ; local environmental noise  $\sigma_l = 0.01$ .

**Figure S13** Influence of ecosystem complexity ( $p_d = 0.1$ ,  $\sigma_h = 1$ ,  $\sigma_l = 1$ )

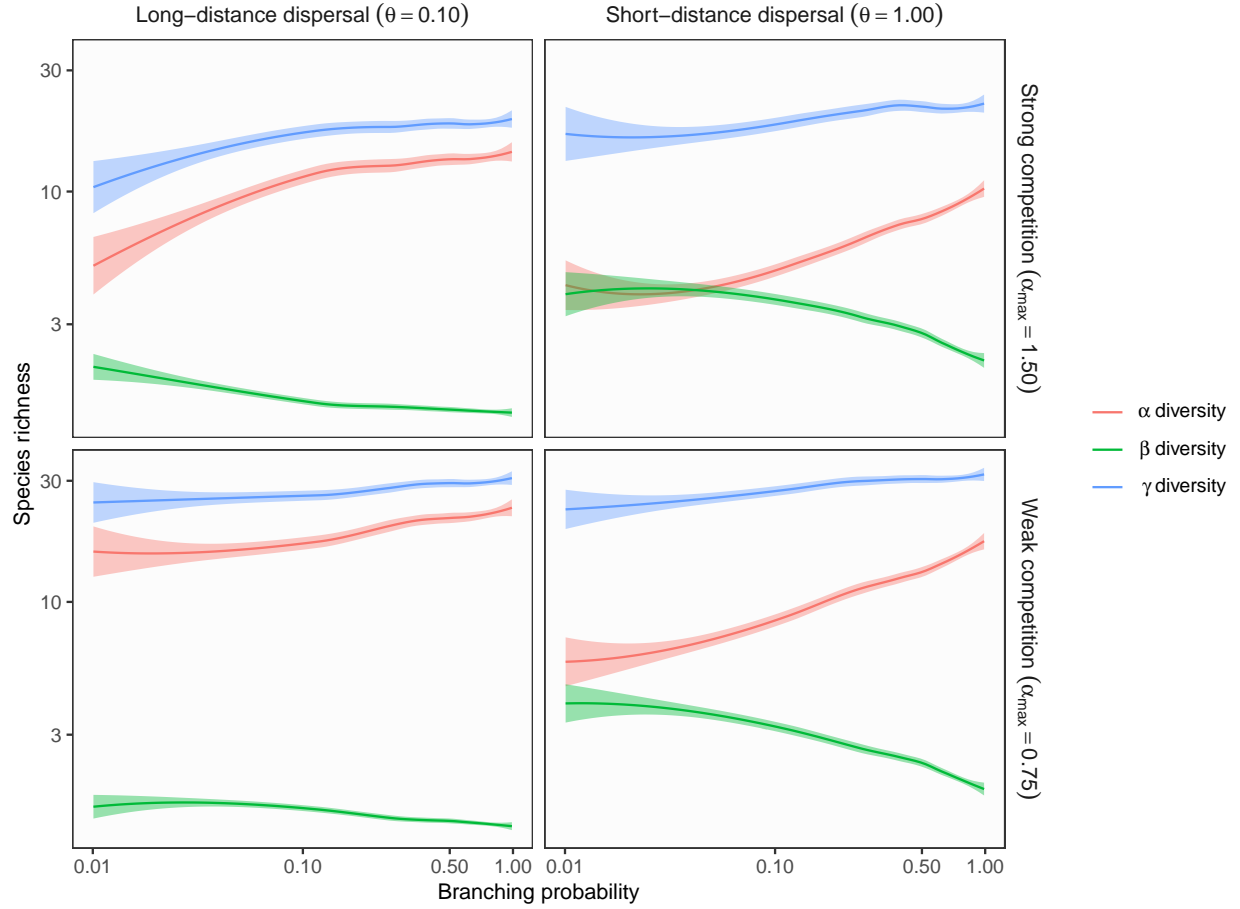


**Figure S13** Theoretical predictions for ecosystem complexity influences (branching probability) on  $\alpha$ ,  $\beta$ , and  $\gamma$  diversity in branching networks. In this simulation, environmental variation at headwaters ( $\sigma_h$ ) is equal to local environmental noise ( $\sigma_l$ ). Lines and shades are loess curves fitted to simulated data and their 95% confidence intervals. Each panel represents different ecological scenarios under which metacommunity dynamics were simulated. Rows represent different competition strength. Competitive coefficients ( $\alpha_{ij}$ ) were varied randomly from 0 to 1.5 (top, strong competition) or 0.75 (bottom, weak competition). Columns represent different dispersal scenarios. Two dispersal parameters were chosen to simulate scenarios with long-distance (the rate parameter of an exponential dispersal kernel  $\theta = 0.10$ ) and short-distance dispersal ( $\theta = 1.0$ ). Other parameters are as follows: dispersal probability  $p_d = 0.1$ ; environmental variation at headwaters  $\sigma_h = 1$ ; local environmental noise  $\sigma_l = 1$ .

**Figure S14 Influence of ecosystem complexity ( $p_d = 0.1$ ,  $\sigma_h = 0.01$ ,  $\sigma_l = 0.01$ )**

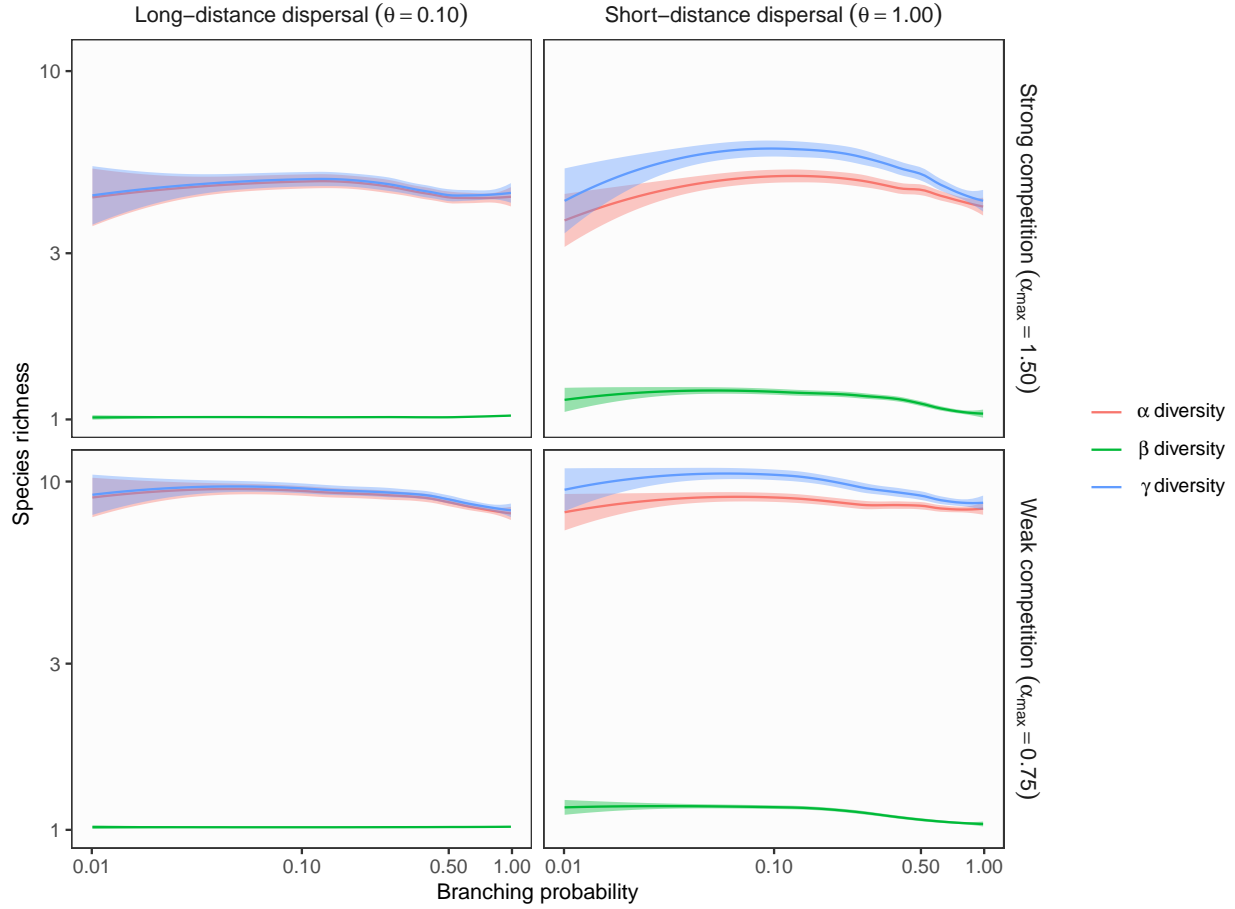


**Figure S14** Theoretical predictions for ecosystem complexity influences (branching probability) on  $\alpha$ ,  $\beta$ , and  $\gamma$  diversity in branching networks. In this simulation, environmental variation at headwaters ( $\sigma_h$ ) is equal to local environmental noise ( $\sigma_l$ ). Lines and shades are loess curves fitted to simulated data and their 95% confidence intervals. Each panel represents different ecological scenarios under which metacommunity dynamics were simulated. Rows represent different competition strength. Competitive coefficients ( $\alpha_{ij}$ ) were varied randomly from 0 to 1.5 (top, strong competition) or 0.75 (bottom, weak competition). Columns represent different dispersal scenarios. Two dispersal parameters were chosen to simulate scenarios with long-distance (the rate parameter of an exponential dispersal kernel  $\theta = 0.10$ ) and short-distance dispersal ( $\theta = 1.0$ ). Other parameters are as follows: dispersal probability  $p_d = 0.1$ ; environmental variation at headwaters  $\sigma_h = 0.01$ ; local environmental noise  $\sigma_l = 0.01$ .

**Figure S15** Influence of ecosystem complexity ( $p_d = 0.1$ ,  $\sigma_h = 0.01$ ,  $\sigma_l = 1$ )

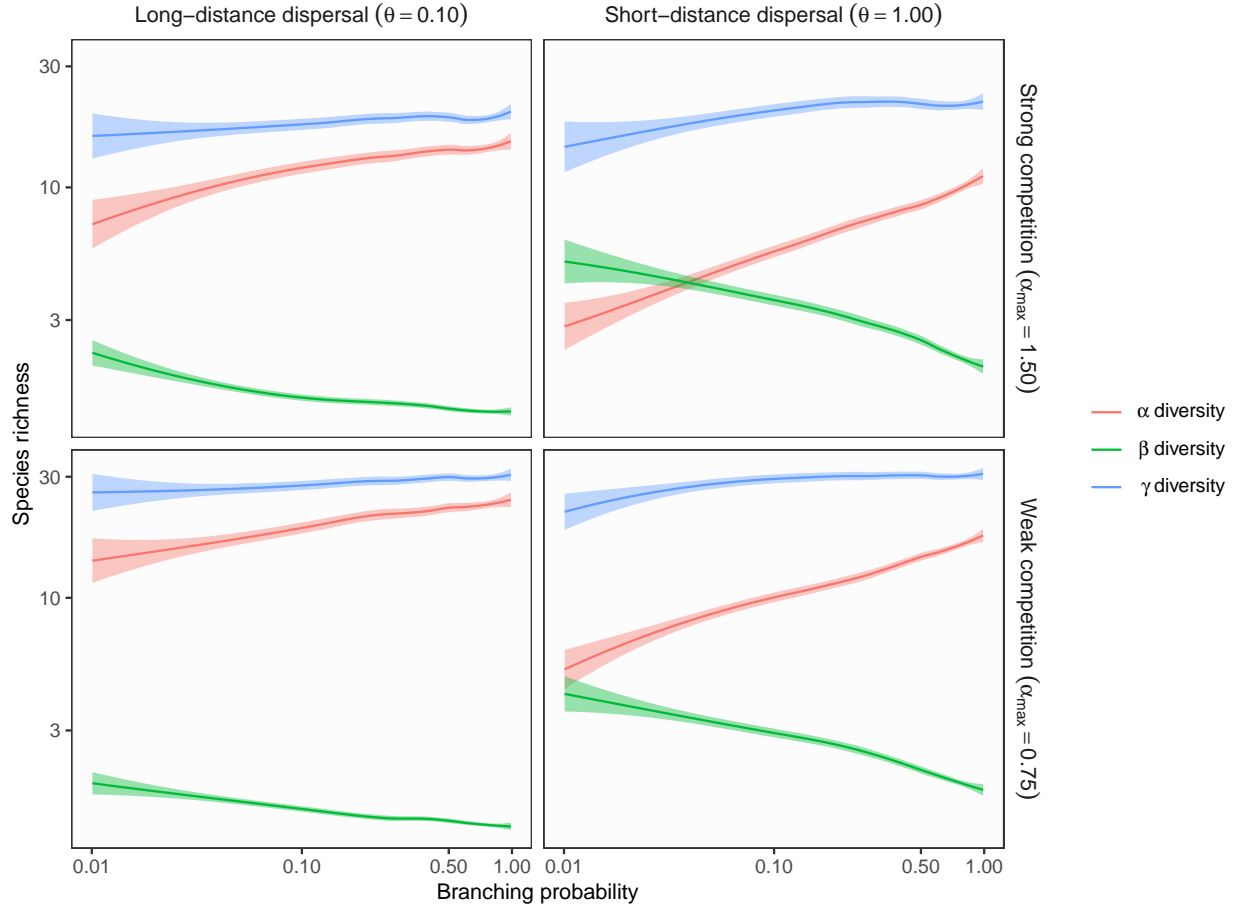


**Figure S15** Theoretical predictions for ecosystem complexity influences (branching probability) on  $\alpha$ ,  $\beta$ , and  $\gamma$  diversity in branching networks. In this simulation, environmental variation at headwaters ( $\sigma_h$ ) is less than local environmental noise ( $\sigma_l$ ). Lines and shades are loess curves fitted to simulated data and their 95% confidence intervals. Each panel represents different ecological scenarios under which metacommunity dynamics were simulated. Rows represent different competition strength. Competitive coefficients ( $\alpha_{ij}$ ) were varied randomly from 0 to 1.5 (top, strong competition) or 0.75 (bottom, weak competition). Columns represent different dispersal scenarios. Two dispersal parameters were chosen to simulate scenarios with long-distance (the rate parameter of an exponential dispersal kernel  $\theta = 0.10$ ) and short-distance dispersal ( $\theta = 1.0$ ). Other parameters are as follows: dispersal probability  $p_d = 0.1$ ; environmental variation at headwaters  $\sigma_h = 0.01$ ; local environmental noise  $\sigma_l = 1$ .

**Figure S16** Influence of ecosystem complexity ( $p_d = 0.01$ ,  $\sigma_h = 1$ ,  $\sigma_l = 1$ )

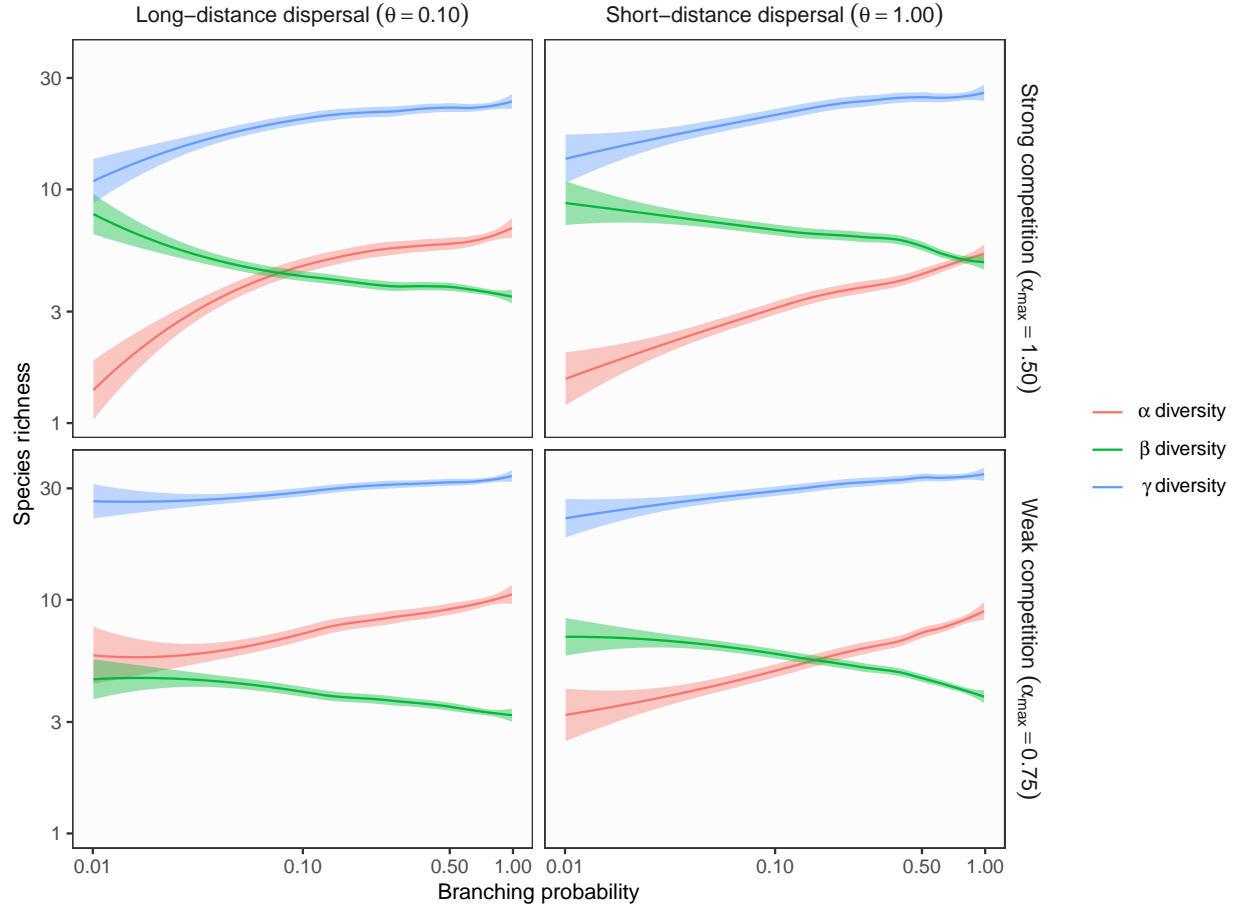


**Figure S16** Theoretical predictions for ecosystem complexity influences (branching probability) on  $\alpha$ ,  $\beta$ , and  $\gamma$  diversity in branching networks. In this simulation, environmental variation at headwaters ( $\sigma_h$ ) is equal to local environmental noise ( $\sigma_l$ ). Lines and shades are loess curves fitted to simulated data and their 95% confidence intervals. Each panel represents different ecological scenarios under which metacommunity dynamics were simulated. Rows represent different competition strength. Competitive coefficients ( $\alpha_{ij}$ ) were varied randomly from 0 to 1.5 (top, strong competition) or 0.75 (bottom, weak competition). Columns represent different dispersal scenarios. Two dispersal parameters were chosen to simulate scenarios with long-distance (the rate parameter of an exponential dispersal kernel  $\theta = 0.10$ ) and short-distance dispersal ( $\theta = 1.0$ ). Other parameters are as follows: dispersal probability  $p_d = 0.01$ ; environmental variation at headwaters  $\sigma_h = 1$ ; local environmental noise  $\sigma_l = 1$ .

**Figure S17 Influence of ecosystem complexity** ( $p_d = 0.01$ ,  $\sigma_h = 0.01$ ,  $\sigma_l = 0.01$ )

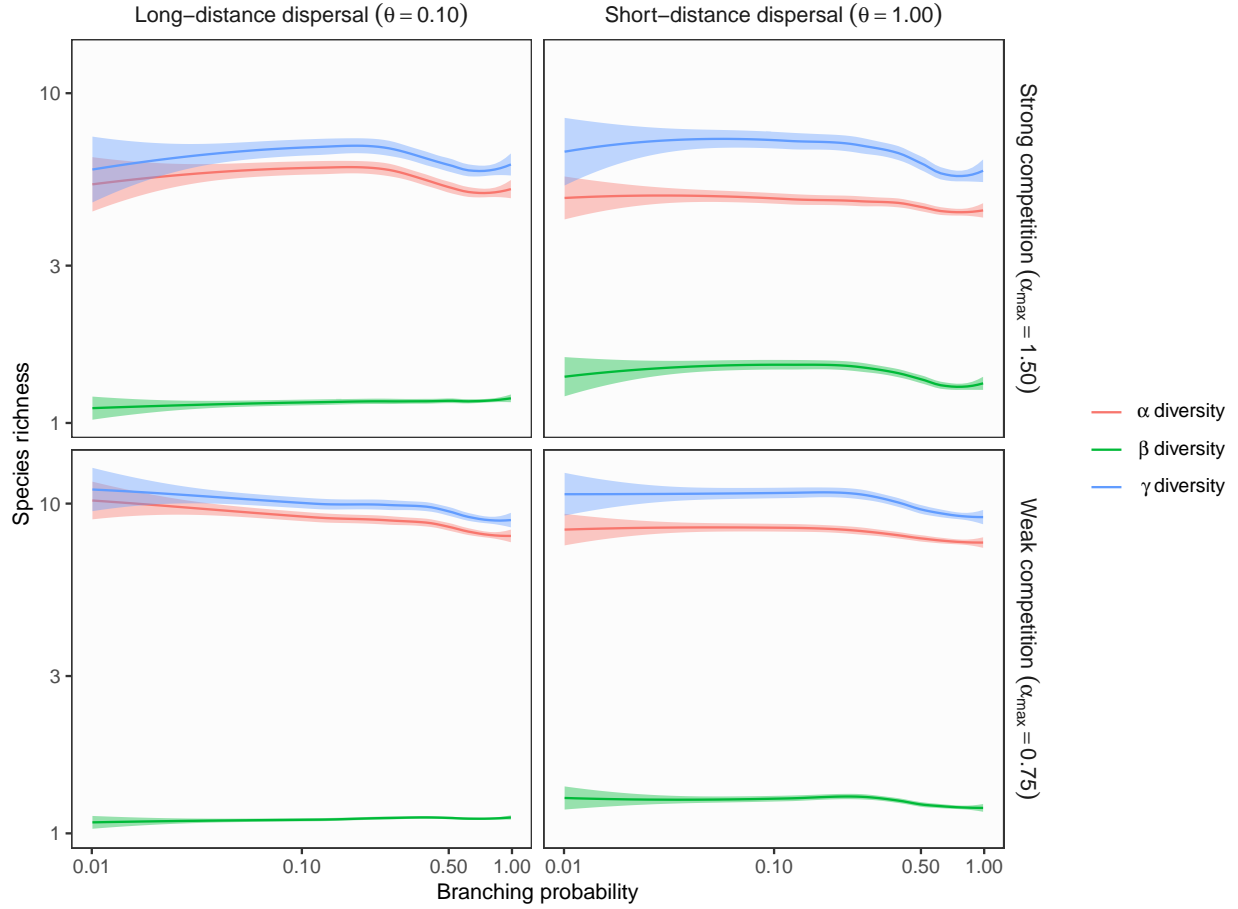


**Figure S17** Theoretical predictions for ecosystem complexity influences (branching probability) on  $\alpha$ ,  $\beta$ , and  $\gamma$  diversity in branching networks. In this simulation, environmental variation at headwaters ( $\sigma_h$ ) is equal to local environmental noise ( $\sigma_l$ ). Lines and shades are loess curves fitted to simulated data and their 95% confidence intervals. Each panel represents different ecological scenarios under which metacommunity dynamics were simulated. Rows represent different competition strength. Competitive coefficients ( $\alpha_{ij}$ ) were varied randomly from 0 to 1.5 (top, strong competition) or 0.75 (bottom, weak competition). Columns represent different dispersal scenarios. Two dispersal parameters were chosen to simulate scenarios with long-distance (the rate parameter of an exponential dispersal kernel  $\theta = 0.10$ ) and short-distance dispersal ( $\theta = 1.0$ ). Other parameters are as follows: dispersal probability  $p_d = 0.01$ ; environmental variation at headwaters  $\sigma_h = 0.01$ ; local environmental noise  $\sigma_l = 0.01$ .

**Figure S18** Influence of ecosystem complexity ( $p_d = 0.01$ ,  $\sigma_h = 0.01$ ,  $\sigma_l = 1$ )

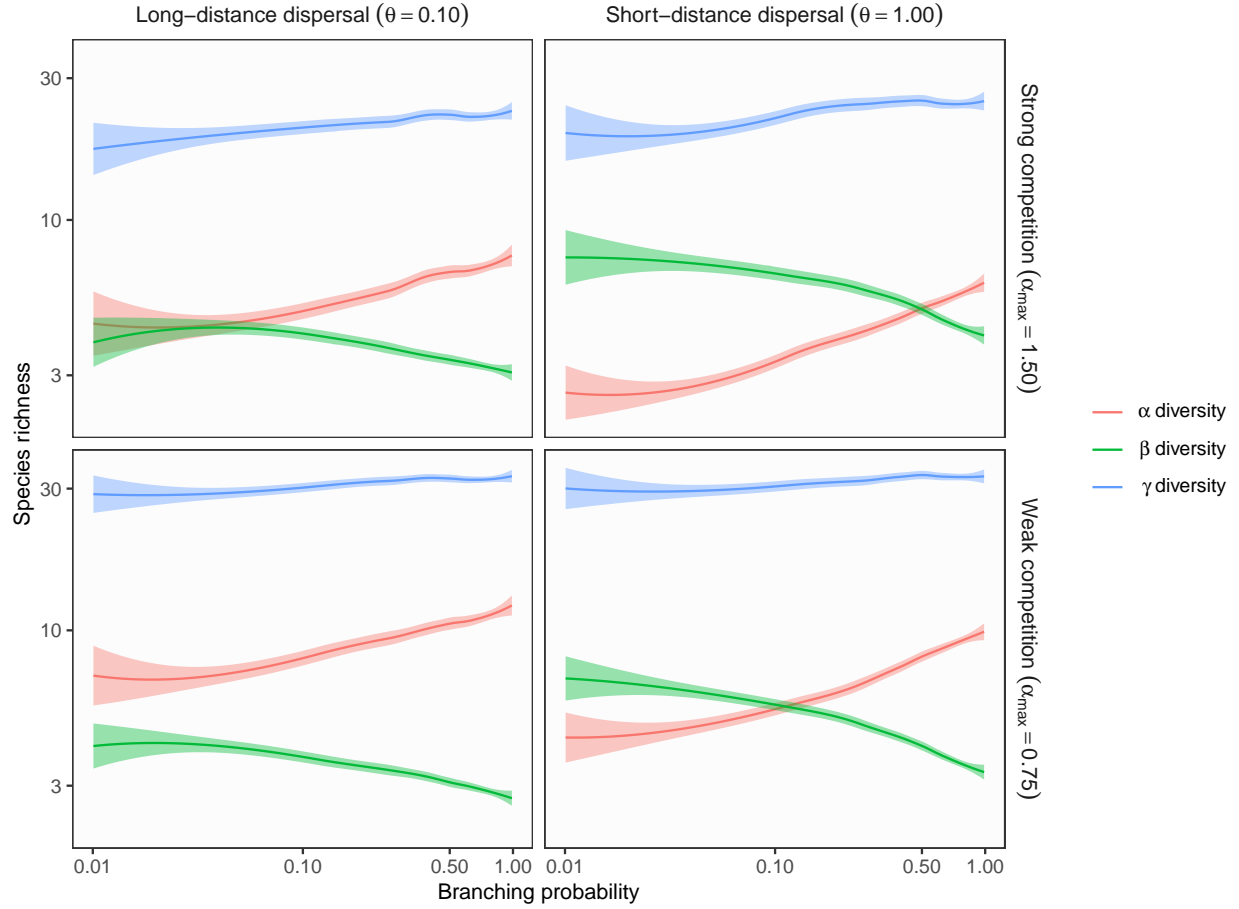


**Figure S18** Theoretical predictions for ecosystem complexity influences (branching probability) on  $\alpha$ ,  $\beta$ , and  $\gamma$  diversity in branching networks. In this simulation, environmental variation at headwaters ( $\sigma_h$ ) is less than local environmental noise ( $\sigma_l$ ). Lines and shades are loess curves fitted to simulated data and their 95% confidence intervals. Each panel represents different ecological scenarios under which metacommunity dynamics were simulated. Rows represent different competition strength. Competitive coefficients ( $\alpha_{ij}$ ) were varied randomly from 0 to 1.5 (top, strong competition) or 0.75 (bottom, weak competition). Columns represent different dispersal scenarios. Two dispersal parameters were chosen to simulate scenarios with long-distance (the rate parameter of an exponential dispersal kernel  $\theta = 0.10$ ) and short-distance dispersal ( $\theta = 1.0$ ). Other parameters are as follows: dispersal probability  $p_d = 0.01$ ; environmental variation at headwaters  $\sigma_h = 0.01$ ; local environmental noise  $\sigma_l = 1$ .



**Figure S19** Correlation structure of explanatory variables

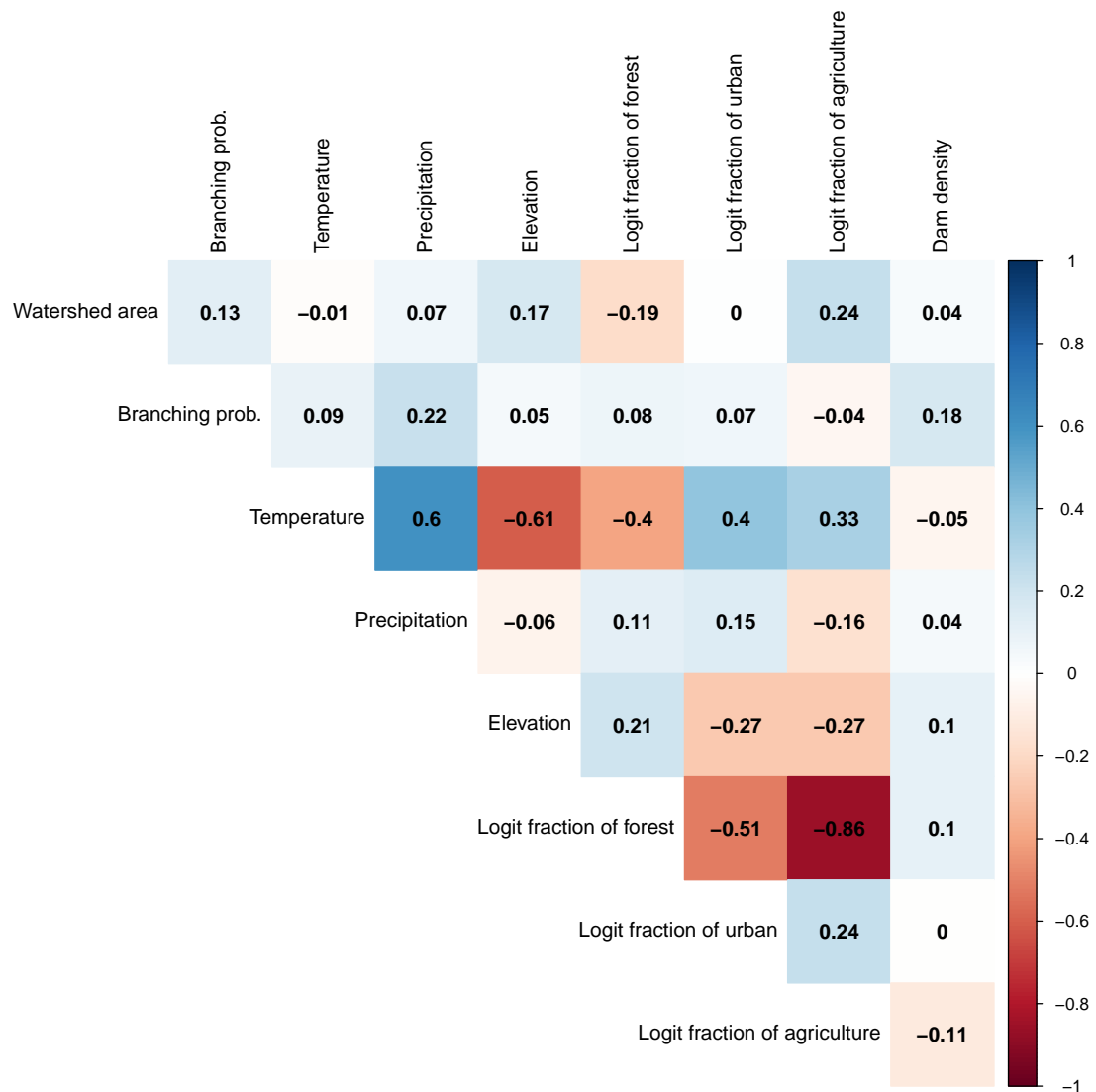


**Figure S19** Correlation structure of potential explanatory variables for riverine diversity metrics. Positive and negative correlations were colored in blue and red, respectively, and darker colors indicate stronger correlations. Environmental variables (temperature, precipitation, elevation, logit fraction of forest, logit fraction of urban, logit fraction of agriculture, and dam density) were expressed as deviations from regional averages to remove any regional effects.

## References

1. McDowall, R. M. Diadromy and the assembly and restoration of riverine fish communities: A downstream view. *Canadian Journal of Fisheries and Aquatic Sciences* **53**, 219–236 (1996).
2. McDowall, R. M. Fighting the flow: Downstream-upstream linkages in the ecology of diadromous fish faunas in West Coast New Zealand rivers. *Freshwater Biology* **40**, 111–122 (1998).
3. Rahel, F. J. & Hubert, W. A. Fish assemblages and habitat gradients in a Rocky Mountain Great Plains stream: Biotic zonation and additive patterns of community change. *Transactions of the American Fisheries Society* **120**, 319–332 (1991).
4. Terui, A. & Miyazaki, Y. Three ecological factors influencing riverine fish diversity in the Shubuto River system, Japan: Habitat capacity, habitat heterogeneity and immigration. *Limnology* **17**, 143–149 (2016).
5. Bsemer, K. *et al.* Headwaters are critical reservoirs of microbial diversity for fluvial networks. *Proceedings of the Royal Society B: Biological Sciences* **280**, 20131760 (2013).
6. Harvey, E., Gounand, I., Fronhofer Emanuel, A. & Altermatt, F. Disturbance reverses classic biodiversity predictions in river-like landscapes. *Proceedings of the Royal Society B: Biological Sciences* **285**, 20182441 (2018).
7. Fukushima, M. Hokkaido Freshwater Fish Database HFish. Center for Environmental Biology and Ecosystem Studies, National Institute for Environmental Studies. (2011).
8. Fukushima, M., Kameyama, S., Kaneko, M., Nakao, K. & Ashley Steel, E. Modelling the effects of dams on freshwater fish distributions in Hokkaido, Japan. *Freshwater Biology* **52**, 1511–1524 (2007).
9. Comte, L. *et al.* RivFishTIME: A global database of fish time-series to study global change ecology in riverine systems. *Global Ecology and Biogeography* **30**, 38–50 (2021).
10. Terui, A. *et al.* Metapopulation stability in branching river networks. *Proceedings of the National Academy of Sciences* **115**, E5963–E5969 (2018).
11. Miyazaki, Y. & Terui, A. Temporal dynamics of fluvial fish community caused by marine amphidromous species in the Shubuto River, southwestern Hokkaido, Japan. *Ichthyological Research* **63**, 173–179 (2016).
12. U. S. Geological Survey and U.S. Department of Agriculture Natural Resources Conservation Service. Federal Standards and Procedures for the National Watershed Boundary Dataset (WBD) (4 ed.): Techniques and Methods 11-A3. (2013).